THE JOURNAL OF COGNITIVE SYSTEMS

an international, peer-reviewed indexed, and open-access periodical

VOLUME 02
NUMBER 01
YEAR 2017
ISSN 2548-0650

www.dergipark.gov.tr/jcs

THE JOURNAL OF
COGNITIVE SYSTEMS

An international, peer-reviewed,
indexed, and open-access periodical

ISSN 2548-0650

AIM & SCOPE

The journal publishes original papers in the field of Cognitive Systems, at large. It accepts contributions by research, as well as by review, and from the field of Cognitive Philosophy. Letter to the editor is also encouraged.

THE JOURNAL OF
COGNITIVE SYSTEMS

CONTACT

Delft University of Technology
Delft, The Netherlands

Istanbul Technical University
Cognitive Systems Lab
Istanbul, Turkey

E-MAIL

cognitive@itu.edu.tr

URL

www.dergipark.gov.tr/jcs

THE JOURNAL OF
COGNITIVE SYSTEMS

VOLUME 02, NUMBER 01

JUNE 2017

CONTENTS

This page is intentionally left blank.

THE JOURNAL OF
COGNITIVE SYSTEMS
VOLUME 02 NUMBER 01 JUNE 2017

EARTHQUAKE HAZARD ANALYSIS FOR DISTRICTS OF DÜZCE VIA AHP AND FUZZY LOGIC METHODS

Levent Sabah[1], Ibrahim Yücedag[1], Cihan Yalcin[2]

[1]Düzce University, Düzce, Turkey
[2]Burdur Office Ministry of Science, Industry and Technology, Burdur, Turkey

Earthquake hazard is defined as the determination of a ground motion from a large earthquake that can cause damage and loss in a certain place and within a certain time period. Damage due to an earthquake is an important element of the earthquake risk concept, which is defined as the probability of loss of property and life. There are many variables that constitute the earthquake hazard. The number and type of these variables may vary in different studies and for different purposes. In this study; geology of the city, lengths of active faults and the epicenter of the earthquake outer-center points of the earthquakes with a magnitude greater than 3 on between 1905 and 2016 were used. In this study; Open Source Code Geographic Information Systems (GIS) Software QGIS, Analytical Hierarchy Process (AHP) and Fuzzy Logic Method have been used to investigate the earthquake hazard of Düzce districts. These parameters were evaluated together to create thematic maps. Regions were determined in terms of earthquake hazard in the generated maps. As a result of the analysis by two methods, the districts showed similar results in terms of earthquake hazard. According to the three criteria evaluated, the central district is the most risky district with 39%. Yigilca, Gölyaka and Kaynaslı districts are medium risky districts. Cilimli, Gümüsova, Cumayeri and Akcakoca are the least risky districts.

Index Terms — Düzce, earthquake hazard analysis, AHP, fuzzy logic, open source code geographic information systems, QGIS, spatial operations

I. INTRODUCTION

93% of our country's soil, 98% of its population and 93% of its dams [1] are in earthquake-affected areas, so the social and economic losses caused by earthquake disaster require very serious precautions [2]. Estimates based on probability calculations in earthquake hazards determinations are important decision tools since the location, timing, magnitude and other features of future earthquakes are uncertain [3].

Earthquake hazard analysis of the settlements is required for taking the precautions. Analyzes should be made using geographic information systems (GIS). Thus, with the thematic maps created together with the spatial and attribute data, scenarios related to pre-disaster, disaster moment and post-disaster can be established with the disaster that can occur. In this context, as a result of the analyzes carried out together with the geographic information systems, priority districts can be determined according to the hazard value. Before any disasters occur, it is possible to achieve the least loss of life and property at the time of disaster and afterwards by carrying out studies aimed at high risk dangerous districts. Geographic information systems can be used to determine the most suitable places for collection areas after disaster.

Manuscript received February 27, 2017; accepted May 25, 2017.
Corresponding author: Levent Sabah (E-mail: leventsabah@duzce.edu.tr; ORCID® ISNI: 0000-0002-6911-4749).
Digital Object Identifier:

II. MATERIALS AND METHODS

The study area includes districts of Düzce. Düzce is plainly located in the western black sea region. The province center of Düzce with an area of 2492 km2 is located at 39051 minutes north latitude and 31008 minutes east longitude. The place of Turkey among the illusions lies in the western and northern part of the Bolu province lands to the east of Sakarya province and the southwestern part of Zonguldak province [4]. The study was conducted in five steps. In the first step, spatial data were used to use in earthquake hazard analysis and to create thematic map in geographic information system. At this step, Düzce provincial boundaries and district boundaries were manually digitized in the form of closed area (polygon) using QGIS open source geographical information system and Google Hybrid map as a base layer. Later active faults and alluvial areas were digitized using the WMS (Web Map Service) published by the General Directorate of Mineral Research and Exploration, "Geoscience Map Viewer and Drawing Editor " [5], as a base layer on QGIS [6]. The epicenter points of earthquakes were obtained by searching the magnitude is greater than or equal 3 through the web page of "B.U. KOERI-RETMC Earthquake Catalog Search System" [7] of Boğaziçi University, Kandilli Observatory and Earthquake Research Institute. The epicenter, which is the earthquake center point, is the point on the earth closest to the focus point. At the same time, it is the point where the earthquake is most damaged or felt the strongest [1]. In the second step, spatial intersection operations were performed using vectorized alluvial areas, active faults, earthquake epicenter point data with Düzce district boundaries using QGIS. Alluvial areas, active faults and earthquake point amounts within the boundaries of each district are thus determined for analysis. In the third step, alluvial areas, active faults and earthquake point data obtained for each district were used as parameters and analyzed with AHP. In the fourth step, alluvial areas, active faults lengths and count of earthquake epicenter point data obtained for each district are used as parameters and analyzed with MATLAB Fuzzy Logic Designer add-on [8]. In the fifth step, based on the earthquake hazard results obtained, thematic maps have been created based on the districts.

A. Preparation of Spatial Data

In the preparation step of spatial data, firstly the province boundaries and districts of Düzce are created by QGIS in the form of vector layer (Figure 1). Afterwards all the vector layers shown in Figure 2 were created. These layers are alluvial areas, active faults and epicenter of the earthquake outer-center points of the earthquakes with a magnitude greater than 3 on between 1905 and 2016.

Fig.1. Creation of Vector Layers with Düzce Province and District Boundaries with QGIS.

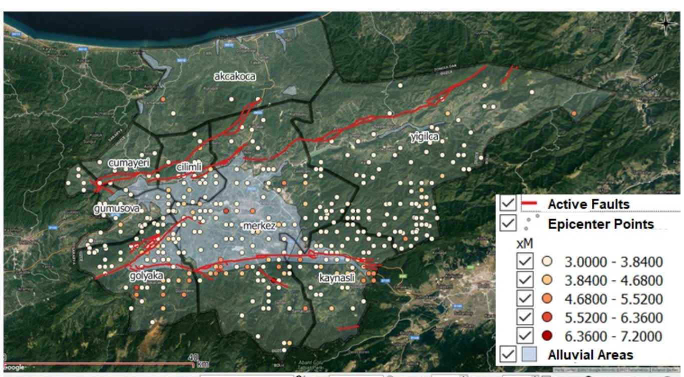

Fig.2. Demonstration of vector layers of epicenter points, active faults and alluvial areas by QGIS for Düzce Earthquake Hazard analysis.

B. Creation of Spatial Data on the Basis of Districts

The layers created in the vector format are intercepted in the QGIS to determine the quantities within each of the boundaries of each district. As a result, new vector layers were created.

C. Earthquake Hazard Analysis with Analytical Hierarchy Process (AHP)

The Analytic Hierarchy Process (AHP) was originally proposed by Myers and Alpert in 1968, and in 1977 it was developed as a model by Saaty to be used in the solution of decision making problems [9]. AHP can be described as a decision-making and forecasting method that gives the percentage distributions of decision points in terms of the factors affecting the decision, which can be used if the decision hierarchy can be defined. The AHP relies on individual benchmarks on a decision hierarchy, using a pre-defined comparison scale, in terms of the factors that influence decision making and, if necessary, the significance of decision points in terms of these factors. As a result, differences in importance are transformed into percentages on decision points [10]. As shown in Figure 3, firstly an aim is determined with the AHP and the criteria are determined accordingly. Subsequently, for each criterion, alternative values are used to obtain values for each alternative. As a criterion epicenter of the earthquake outer-center points of the earthquakes with a magnitude greater than 3, active faults lengths and alluvial areas were used for each district boundary to determine the earthquake hazard. Alternatively, the districts are used. Thus, appropriate earthquake hazard results were obtained by using the values of the three criteria each ruler had. The values used for each district in the AHP analysis are shown in Table I. The values obtained as the result of the analysis are shown in Table II. As a result of the analysis, it is seen that the central district has the highest earthquake hazard value.

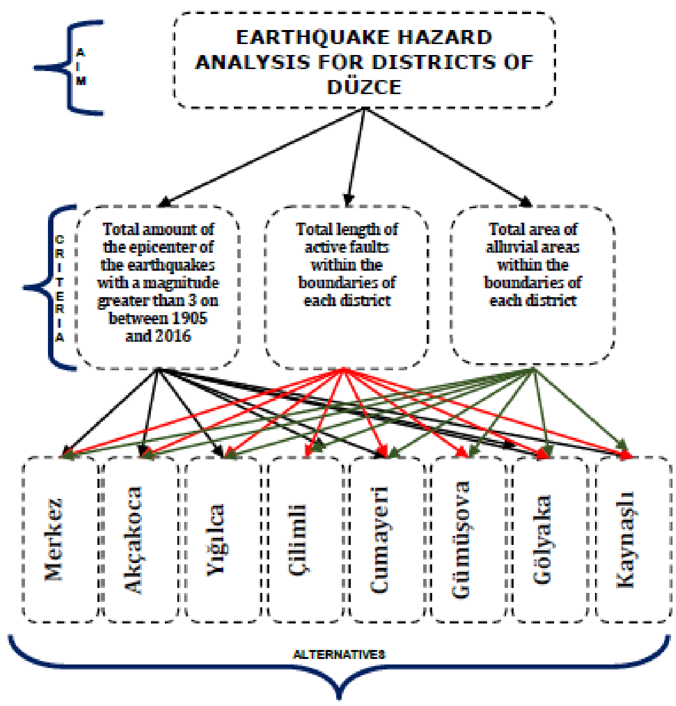

Fig 3. General Structure of AHP.

Table I. Epicenter of the earthquakes with a magnitude greater than 3, active faults lengths and alluvial areas were used for each district boundary values

Districts	Epicenters >= 3 (total)	Active Faults (m)	Alluvial Areas (km²)
Akçakoca	4	6593	24.020
Yığılca	96	66661	7.445
Çilimli	24	27619	46.401
Cumayeri	14	22855	10.983
Gümüşova	33	8575	24.842
Gölyaka	72	46472	46.664
Kaynaşlı	68	32143	47.294
Merkez	142	80405	323.785

Table II. Earthquake Hazard Values of Düzce Districts as a Result of Analysis with AHP

District	Rank	AHP Values (%)
Merkez	1	39.55
Yığılca	2	15.00
Gölyaka	3	13.40
Kaynaşlı	4	11.53
Çilimli	5	07.75
Gümüşova	6	04.91
Cumayeri	7	04.29
Akçakoca	8	02.52

The thematic map of the analysis values is shown in Figure 4. The hazard value is increasing towards the southern parts of Düzce province. The hazard values of the earthquake towards the red tone from the blue tones are increasing.

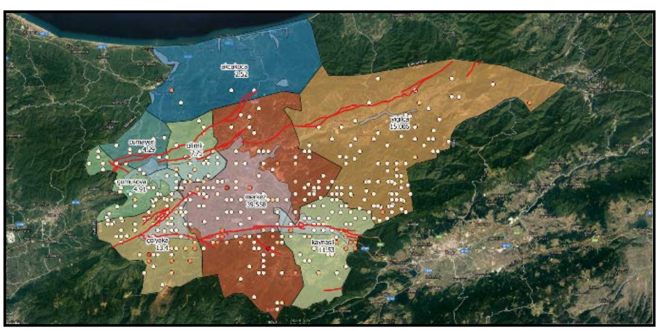

Fig.4. Demonstration of AHP Earthquake Hazard Values of Düzce Districts with Thematic Map by QGIS

D. EARTHQUAKE HAZARD ANALYSIS WITH FUZZY LOGIC

Fuzzy logic is a concept that first appeared in 1965 when Dr. Lotfi A. Zadeh published an article on "Information and Control" in this issue. Fuzzy logic is a very valuable form of logic that deals with values that are roughly characterized and can be reasonably judged from absolute and exact values [11]. Fuzzy logic holds intermediate values such as very long, long, medium, short, and very short instead of long-short, as in human logic, and everything is represented by values in the range [0,1]. In summary, fuzzy logic is preferred if the results in a system need not be precisely defined, if the results are to be displayed in range values, or if mathematical criteria are to be determined and classified as adjectives [11 - 18]. The reason of comparison fuzzy logic with AHP is time and location of the disaster is uncertain. Using fuzzy logic method, a model with current data is created. In this model, earthquake hazard is defined as low, medium and high. After the earthquake disaster, the fuzzy logic model will be used to model the current earthquake hazard values only by entering the current system.

In the Fuzzy Logic Method, criterion values are used in a similar manner to the AHP method. For this, Fuzzy Logic Designer plugin is used via MATLAB. Membership functions were created separately for each criterion to reach the results obtained in the AHP with the existing values. Afterwards, the basic rule table is defined, for example, if the number of epicenter points, the fault length and the alluvium area of a district are low, earthquake hazard is low and in the opposite case, the danger value is high. Furthermore, the decision maker has been defined according to various probability interpretations of the rule table. All rules were evaluated and earthquake hazard analysis was made according to the values that each district had. Figure 5 shows the general structure of the fuzzy logic model. From the left to the right in the direction of flow, firstly the rules are added to the rule table which is created together with the values that the districts have for each criterion.

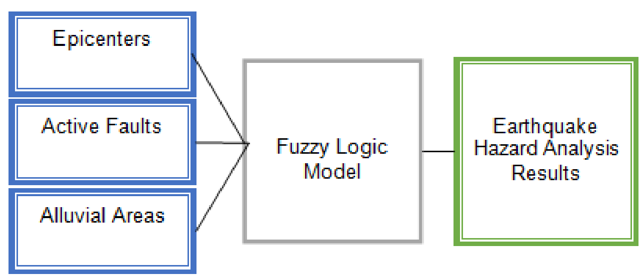

Fig.5. General structure of Fuzzy Logic.

The values used in the generated fuzzy logic model are as in Table III.

Table III. Input and Output Values Used in Fuzzy Logic Model

	Range	Low	Medium	High
Epicenters (Figure 6)	[0 200]	[0 0 8 55]	[16.5 55.8 117]	[55 168 200 200]
Active Faults (Figure 7)	[0 120]	[0 0 7.2 40]	[0 0 7.2 40]	[0 0 7.2 40]
Alluvial Areas (Figure 8)	[0 400]	[0 0 11 66]	[0 73.2 149.1]	[66 191.4 400 400]
Earthquake Hazard Results (Figure 9)	[0 30]	[0 0 0.0348 5.25]	[2.303 5.518 6.533 10.2]	[5.3 16.2 30.3 30.3]

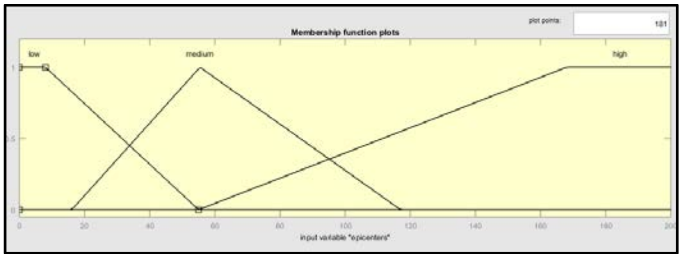

Fig.6. Membership Function of Earthquake Epicenter Points Data

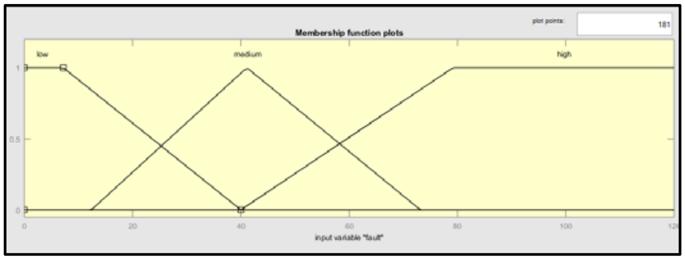

Fig.7. Membership Function of Active Faults Data

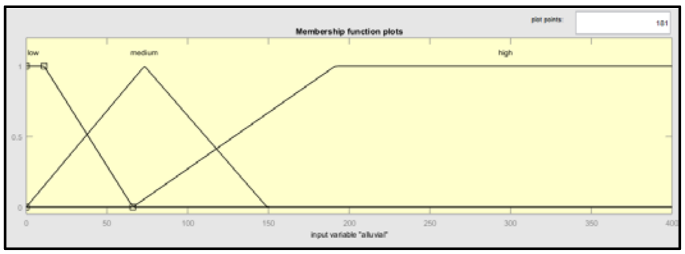

Fig.8. Membership Function of Alluvial Areas Data

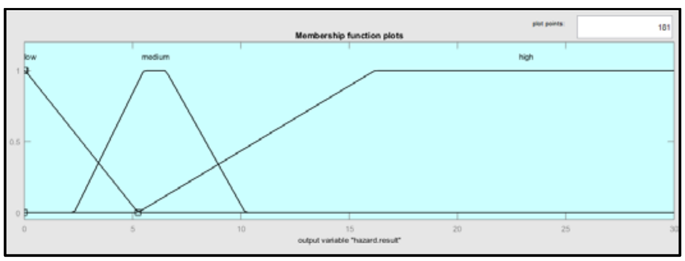

Fig.9. Membership Function of MATLAB Fuzzy Logic Designer Results

1. If (epicenters is low) and (fault is low) and (alluvial is low) then (hazard.result is low) (1)
2. If (epicenters is high) and (fault is high) and (alluvial is high) then (hazard.result is high) (1)
3. If (epicenters is medium) and (fault is medium) and (alluvial is medium) then (hazard.result is medium) (0.8)
4. If (epicenters is medium) and (fault is medium) and (alluvial is low) then (hazard.result is medium) (0.2)
5. If (epicenters is low) and (fault is medium) and (alluvial is low) then (hazard.result is low) (0.5)
6. If (epicenters is medium) and (fault is low) and (alluvial is low) then (hazard.result is low) (0.5)

Fig.10. Rule Table

After the fuzzy model is constructed, the earthquake hazard values obtained according to the input values are obtained visually with the rule viewer. In Figure 11, the hazard result values change dynamically according to the values obtained by moving the vertical red line with the mouse to the right or left by hand. The earthquake hazard value of 18.80 is obtained, which is count of epicenter of the earthquakes with a magnitude greater than 3 is 100, length of faults is 60 km and alluvial area is 200

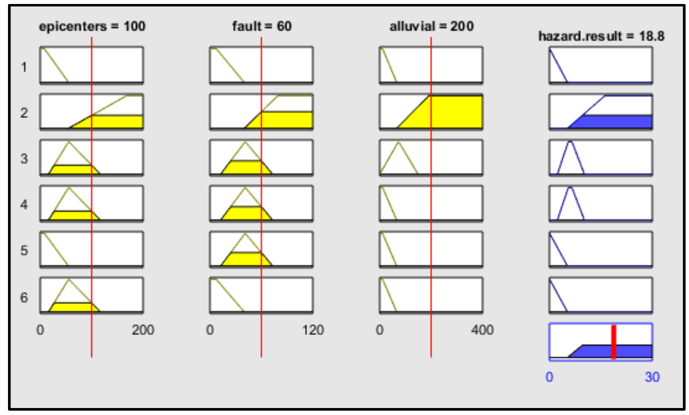

Fig.11. Visual View of Rule Table.

km². This value should be multiplied by 2 to normalize with AHP results. Equivalent AHP value is 37.60%. While the basic rule table was constructed, the values of each districts were evaluated separately for each criterion. Values close to those obtained with AHP were found. In this way, earthquake hazard analysis can be performed quickly with the values to be entered via MATLAB with the dynamically changing numbers.

III. FINDINGS AND DISCUSSION

The results obtained by using AHP and Fuzzy Logic methods are shown in Table 4. In Figure 12, the results obtained from AHP and Fuzzy Logic Model for each district is similar to the correlation value of 0.996.

Table.4. Earthquake Hazard Values Obtained with AHP and Fuzzy Logic Models of Düzce Districts.

District	Rank	AHP Values (%)	Fuzzy Logic Values	Fuzzy Logic Values * 2 (%)
Merkez	1	39.55	19.70	39.40
Yığılca	2	15.00	06.24	12.48
Gölyaka	3	13.40	06.20	12.40
Kaynaşlı	4	11.53	05.73	11.46
Çilimli	5	07.75	03.87	07.74
Gümüşova	6	04.91	02.00	04.00
Cumayeri	7	04.29	01.92	03.84
Akçakoca	8	02.52	01.75	03.50

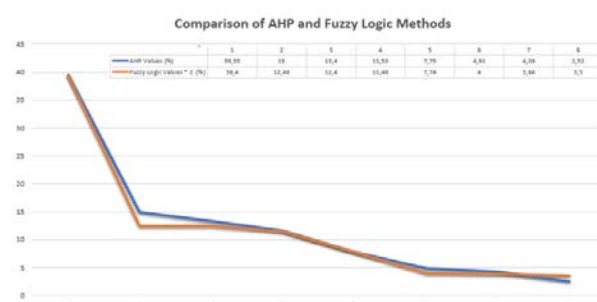

Fig.12. Demonstration of Results Obtained by Using AHP and Fuzzy Logic Methods.

IV. RESULTS AND RECOMMENDATIONS

Accelerating and analyzing earthquake hazard analysis is possible by evaluating several parameters. With AHP and Fuzzy Logic methods, earthquake hazard analysis can be done and the results are compatible with each other. According to the three criteria, earthquake hazard analysis for Düzce central district is the most risky district with 39% .Yığılca, Gölyaka and Kaynaşlı districts are medium risky districts. Çilimli, Gümüşova, Cumayeri and Akçakoca were determined as the least risky districts. The use of fuzzy logic for a dynamic earthquake hazard model is a quick solution. In the classical AHP Method, post-disaster values are re-adding and recalculations for each criteria and alternatives. In the fuzzy logic, after post-disaster only changed values of criteria or alternatives are updating via MATLAB fuzzy logic extension and then updated earthquake hazard analysis results can be obtained.

ACKNOWLEDGMENT

The study is selected from International Engineering Research Symposium-UMAS 2017 (Duzce University).

REFERENCES

[1] http://www.koeri.boun.edu.tr/sismo/Personel/comoglu/depremnedir ,07/07/2017

[2] Bayındırlık Ve İskan Bakanlığı Deprem Şurası Sonuç Bildirgesi, İstanbul, 1 Ekim 2004

[3] F. Özçep, M. Aşçı, N. Alpaslan, T. Yas, D. Gündoğdu, "Statik Ve Dinamik (Deprem) Etkiler Altında Zemin Davranışı", Deprem Sempozyumu, Kocaeli, 2005

[4] Düzce Organize Sanayi Bölgesi Revizyon İmar Planı 1/5000 – 1/1000 Açıklama Raporu, 2017

[5] http://yerbilimleri.mta.gov.tr/anasayfa.aspx, 07.11.2017

[6] http://www.qgis.org/tr/site, 07.11.2017

[7] http://udim.koeri.boun.edu.tr/zeqdb, 07.11.2017

[8] https://www.mathworks.com/help/fuzzy/fuzzylogicdesigner-app.html?requestedDomain=www.mathworks.com , 07/07/2017

[9] S. Uzun, H. Kazan, "Çok Kriterli Karar Verme Yöntemlerinden AHP TOPSIS ve PROMETHEE Karşılaştırılması: Gemi İnşada Ana Makine Seçimi Uygulaması", Journal of Transportation and Logistics, 2016

[10] http://debis.deu.edu.tr/userweb/k.yaralioglu/dosyalar/ Analitik_Hiyerarsi_Proses.doc, 05.07.2017

[11] F. Bozyiğit, D. Kılınç, A. Kut, M. Kaya, "Bulanık Mantık Algoritmaları Kullanarak Kaynak Kod Benzerliği Bulma", XVII. Akademik Bilişim Konferansı – Ab, 2015

[12] M. Yılmaz, E. Arslan, "Bulanık Mantığın Jeodezik Problemlerin Çözümünde Kullanılması", Harita ve Kadastro Mühendisleri Odası, Mühendislik Ölçmeleri STB Komisyonu 2. Mühendislik Ölçmeleri Sempozyumu, 23-25 Kasım 2005, İTÜ – İstanbul

[13] M.A. Derinpınar, A. Ç. Aydınoğlu, "Bulanık Mantık ile Coğrafi Bilgi Teknolojilerini Kullanarak Taşınmaz Değerlemesi", TMMOB Harita ve Kadastro Mühendisleri Odası, 15. Türkiye Harita Bilimsel ve Teknik Kurultayı, 25-28 Mart 2015, Ankara

[14]C. Şenol, T. Yıldırım, "Bulanık-Sinir Ağı Yapısı İçin Yeni Bir Karma Yaklaşım", http://www.emo.org.tr/ekler/2d3d18a536479e3_ek.pdf

[15] İ. Y. Kazu , O. Özdemir, "Öğrencilerin Bireysel Özelliklerinin Yapay Zeka ile Belirlenmesi (Bulanık Mantık Örneği)", Akademik Bilişim 09 - XI. Akademik Bilişim Konferansı Bildirileri 11-13 Şubat 2009 Harran Üniversitesi, Şanlıurfa

[16] B. Gültekin, S. Biroğul, İ. Yücedağ, "İşe Alım Süreci Aday Ön Tesbitinde Bulanık Mantık Tabanlı SQL Sorgulama Yönteminin İncelenmesi", Düzce Üniversitesi Bilim ve Teknoloji Dergisi, 3 (2015) 198-209

[17] M. E. Bayrakdar, S. Bayrakdar, İ. Yücedağ, A. Çalhan, "Bilişsel Radyo Kullanıcıları için Bulanık Mantık Yardımıyla Kanal Kullanım Olasılığı Hesabında Farklı Bir Yaklaşım", Düzce Üniversitesi Bilim ve Teknoloji Dergisi, 3 (2015) 88-99

[18] M. Ş. Biçen,, A. Çalhan, İ. Yücedağ , "Kablosuz Heterojen Algılayıcı Ağlarda Bulanık Mantık Tabanlı Ağ Geçidi Seçimi", Düzce Üniversitesi Bilim ve Teknoloji Dergisi, 4 (2016) 655-660

BIOGRAPHIES

Levent Sabah was born in Eskişehir, Turkey. He received the B.Sc. degree in Computer Engineering from Çukurova University, Adana, Turkey, in 2011. Since 2017 he has been working at Düzce University, as a specialist at the IT department. Currently he is finalizing his master studies in Computer Engineering, Düzce Üniversity. His current research interests are R programming, big data, data mining, social network analysis, geographic information systems, augmented reality and mobile application development.

İbrahim Yücedağ received the B.Sc., M.Sc., and Ph.D. degrees from Gazi University, Ankara, Turkey, in 1995, 1998, and 2007, respectively. He is currently an Associate Professor with the Department of Computer Engineering, Düzce University.

Cihan Yalçın received the B.Sc. degree in Geological Engineering from Selçuk University, Konya, Turkey, in 2009 and M.Sc. degree from Kahramanmaraş Sütçü İmam Üniversity, in 2012. He worked as a Reserach Asistant at Kahramanmaraş Sütçü İmam University between 2010-2012. Since 2012 he has been working at Ministry Of Science, Industry and Technology as an engineering. Currently he is continuing his Phd Studies at Istanbul University.

THE JOURNAL OF
COGNITIVE SYSTEMS
VOLUME 02 NUMBER 01 JUNE 2017

CLASSIFICATION OF EPILEPTIC AND HEALTHY INDIVIDUALS WITH RECURRENCE PARAMETERS

Funda Kutlu Onay[1], Cemal Kose[2]

[1] Amasya University, Amasya, Turkey
[2] Karadeniz Technical University, Trabzon, Turkey

Epilepsy is a brain activity disorder that manifests itself with epileptic seizures. Although the reasons of epilepsy are not fully known, the diversity and variability of the individual make it difficult to diagnose epilepsy. For this, the diagnosis of epilepsy with computerized systems is one of the most popular research topics in recent years. Although many techniques and methods have been developed for this purpose, Electroencephalogram (EEG) signals are one of the most preferred and most basic ways to diagnose epileptic seizures or epilepsies because of their practicality and easy application. However, interpretation of EEG signals is not easy due to nonlinear and variable signal characteristics. This has led to the preference of nonlinear methods as well as traditional methods in the study of EEG signals. It can be seen from the literature that non-linear methods give very successful results in previous studies. In this study; EEG signals from healthy and epileptic subjects were represented by recurrence parameters obtained by recurrence plot. The features extracted from the recurrence plot are applied to multi-layered artificial neural networks, k-nearest neighbors, and support vector machines classifiers after feature selection process. Accordingly, the highest classification accuracy was achieved at around 97.05% when the multi-layered artificial neural network was used.

Index Terms—recurrence parameters, recurrence quantification analysis, EEG, epilepsy, non-linear classification

I. INTRODUCTION

COMPUTER-ASSISTED disease diagnosis is one of the most studied areas on the present day. Thanks to the developed software, misdiagnosis of diseases is reduced and the time for diagnosis is shortened. One of the most common areas of use of this technology is the diagnosis of epilepsy.

Epilepsy is a disorder of brain dysfunction that occurs in the form of recurrent seizures and affects about 1% of the world's population [1]. Epilepsy affects human life seriously because it causes depression, anxiety disorders, psychosis in adults and deficiency, hyperactivity, stuttering in children. [2]. As a result, epilepsy has an important position in biomedical researches for many years. The reasons of epilepsy are not known exactly, but the human brain has the potential to have epileptic seizures, even with neurological damages such as head trauma, high fever. Today, approximately 30,000 new epilepsy patients are attending annually, and about 30% of them are children under the age of 18. It is known that approximately 720.000 individuals in Turkey are suffering from epilepsy [3].

Epilepsy is commonly seen in mammalian species due to their complex brain structures [1]. More than 40 types of seizures have been described in the literature. For this reason, epileptic seizures are difficult to perceive and it takes a long time to find the source of the problem. In fact, since symptoms from other ailments are sometimes interpreted as epileptic seizures, BCI systems have begun to be developed to prevent the misdiagnosis of diseases [2].

The human brain continuously generates an electrical current at low voltage. These signals, which are mostly transmitted in a computer environment as EEG or ECoG signals, are used for automatic diagnosis and computer analysis for epilepsy or other purposes. Due to the non-invasive, practical availability and ease of application, EEG signals are the most preferred signals in BCI applications. Due to non-periodic and non-stationary characteristics and unstable amplitude, phase, and frequency values, interpretation of EEG signals are difficult. As such, there is a great need for the development of efficient automated methods and systems for EEG analysis [4].

In this study, the EEG data set was used which is recorded by Bonn University for the detection of epilepsy and perception of epileptic seizures. These data were recorded from 100 channels for 23.6 sec, with 5 healthy and 5 epileptic patients. Each trial has three periods: normal, pre-seizure, and seizure [5]. There are successful studies in the literature where this data set is used. Gautama et al. utilized nonlinear methods to represent normal and epileptic EEG signals and attained 86.2% classification accuracy [6]. Kannathal et al. achieved 90% classification accuracy using entropy and adaptive fuzzy logic interference system [7]. Tzallas et al. studied using time-frequency analysis and k-EYK classifier and obtained 97.71-100% success rate [8]. Polat and Güneş acquired 98% classification accuracy with decision trees and fast Fourier transformation based systems [9]. Acharya achieved 97.7%

Manuscript received May 5, 2017; accepted May 25, 2017.
Corresponding author: Funda Kutlu Onay (E-mail: funda.kutlu@amasya.edu.tr; ORCID® ISNI: 0000-0002-8531-4054).
Digital Object Identifier:

and 94.7% classification accuracy using RQA with SVM and Fuzzy classifiers, respectively [10].

II. DATASET DESCRIPTION AND PROPERTIES

The dataset used in the study is an EEG database recorded in the Epileptology Department of the University of Bonn in Germany and open to public access. This data was recorded with a 128-channel 12-bit EEG recording system and sampled with a sampling frequency of 173.61. Therefore, each experiment is 23.6 seconds long. There are a total of 500 trials in this way and these were taken from 5 groups (A, B, C, D, E). The experimental groups, explanations, and trial numbers are given in Table I. All experiments are free of physical artifacts caused by eye and muscle movements [5].

Table I. Information of experimental groups

Groups	Explanation	Trial numbers
A	Eyes open from healthy individuals	100
B	Eyes closed from healthy individuals	100
C	Seizure-free from hippocampal formation of the opposite hemisphere of the brain	100
D	Seizure-free from epileptic zone	100
E	Seizure activity	100

EEG signals were recorded from volunteers according to the international 10-20 electrode placement system. A sample test of each of the experimental groups is given in figure 1, as A-B-C-D-E, respectively.

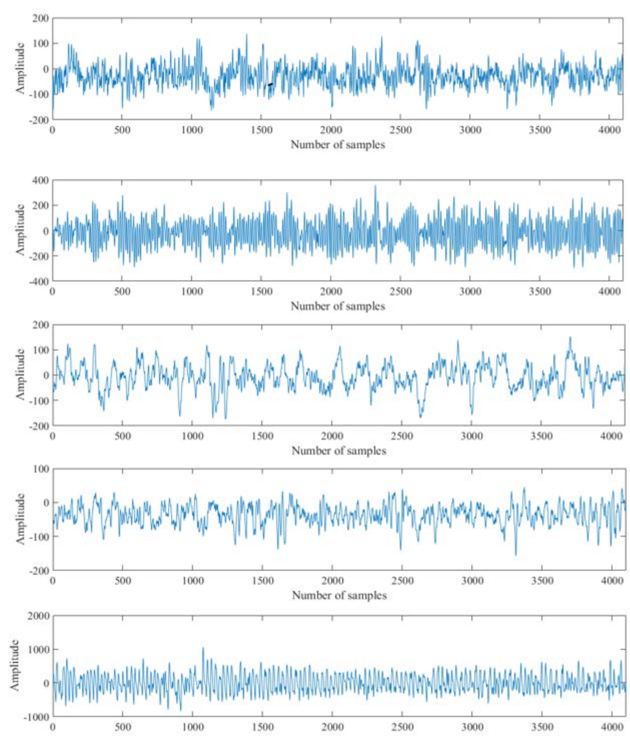

Fig. 1. Sample EEG signals for A, B, C, D, and E, respectively.

III. FEATURE EXTRACTION AND SELECTION

Recurrence quantification analysis (RQA) is a method used by Eckmann [11] to analyze nonlinear data [11]. It is possible to pick out the dynamic areas and to detect the nonlinear states on the signal with RQA parameters extracted from the recurrence plot (RP). Since EEG signals also have these characteristic features, RQA has become a frequently used method in the analysis of EEG signals. The mathematical equation used in RP calculation is given as

$$R_{i,j} = \Theta\left(\varepsilon_i - \|x_i - x_j\|\right), \quad x_i \in \Re^m, \quad i,j = 1\ldots N, \tag{1}$$

The RQA metrics obtained from RP are explained in Table II. Here, ||.|| corresponds to Euclidean distance; x_i , points to the considered point and N is the total number of points to be considered. ε_i is the predetermined threshold distance and, θ_i Heaviside step function and is defined as

$$\Theta = \begin{cases} 1 \, if \; s \geq 0 \\ 0 \, if \; s < 0 \end{cases} \tag{2}$$

Table II. Description of RQA parameters

RQA parameters	Equation	Description
Recurrence Rate (RR)	$RR = \frac{1}{N^2}\sum_{i,j=1}^{N} R_{i,j}$	It gives the density of repetitive points in RP. Corresponds to the sum of the correlations.
Determinism (DET)	$DET = \frac{\sum_{l=l\min}^{N} lP(l)}{\sum_{i,j}^{N} R_{i,j}}$	Corresponds to the percentage of repetition points located on the diagonals.
Laminarity (LAM)	$LAM = \frac{\sum_{v=v\min}^{N} vP(v)}{\sum_{v=1}^{N} vP(v)}$	Corresponds to the percentage of repeat points located on the vertical line.
L	$L = \frac{\sum_{l=l\min}^{N} lP(l)}{\sum_{l=l\min}^{N} P(l)}$	Average diagonal line length
Trapping time (TT)	$TT = \frac{\sum_{v=v\min}^{N} vP(v)}{\sum_{v=v\min}^{N} P(v)}$	Average vertical line length
Selective Entropy (ENTR)	$ENTR = -\sum_{l=l\min}^{N} p(l)\ln p(l$	

There are three important parameters for the creation of the correct and most selective RP: embedding dimension, time delay and threshold. False Nearest Neighbor (FNN) was used in determining the best embedding dimension parameter in the study and was found as 7 for healthy individuals and as 6 for epileptic individuals. The Mutual Information (MI) algorithm was applied to find the best time delay parameter and was obtained as 4 for healthy individuals and as 3 for epileptic individuals. The healthy and epileptic RPs generated by these parameters are given in figure 2-a and figure 2-b, respectively.

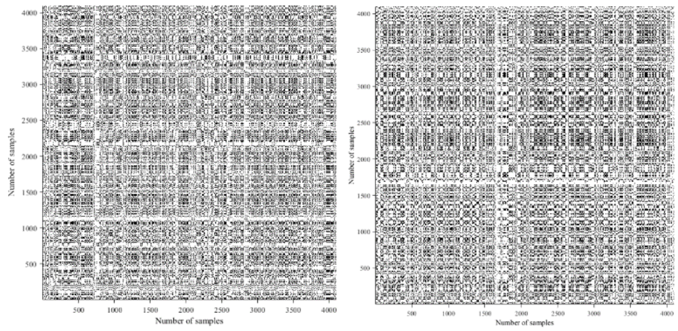

Fig. 2. Samples RPs for a) healthy b)epileptic

Feature selection is a process performed to determine the properties that best represent the class within a feature set. In order to increase classification performance, the features that do not contain enough information about the class are eliminated by feature selection algorithms. In this study, the feature selection process was performed by Chi-square method. Chi-square is a hypothesis testing method that tests the dependency and independence between two variables. The feature selection based chi-square testing consists of two steps. In the first part of the method, the Chi-square statistics of the attributes are calculated according to the class characteristic. In the second phase, the attributes are decomposed until the inconsistent features in the dataset are determined by looking at the Chi-square values in the Chi-Merge principle, depending on the degree of freedom and the level of significance determined. The Chi-square value for an instance in the dataset indicates the dependency of this in the class. If this value is zero, the instance is independent within that class; if it is a high value, this example is more specific for the data set [12]. The mathematical equation used to calculate the Chi-square value is given as

$$\chi^2 = \sum_{i=1}^{2}\sum_{j=1}^{k}\frac{(A_{ij}-E_{ij})}{E_{ij}} \qquad (3)$$

According to this equation, k is the number of classes, A_{ij} (i, row, j, column) is the measured frequency value and E_{ij} is the expected frequency value.

The feature vector obtained after the feature selection process is applied to the classifiers. The classifiers used in the next section will be mentioned.

IV. CLASSIFICATION

A. MULTILAYER ARTIFICIAL NEURAL NETWORKS (MLANN)

Artificial neural network is a classification technique inspired by the work of the human brain and is based on learning. The human brain has the ability to learn events and make inferences from these events, and ANN studies are simulated by models of neural networks in the brain. The task of an ANN is to specify the set of outputs that correspond to a given set of inputs [13]. MLANN is a neural network model consisting of one or more layers. A MLANN consists of three basic layers: an input layer that serves data, a hidden layer (or more) that best separation between classes and an output layer that reveals class information about the input value. An example of a MLANN structure is given in figure 3.

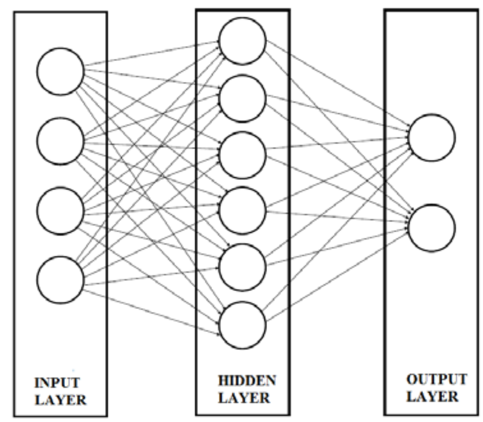

Fig. 3. Illustration of a MLANN architecture

The neurons in the hidden layer(s) detect features. For this reason, the number of layers and neurons in the hidden layer(s) are important parameters for the best separation. Apart from this, learning coefficient and momentum coefficient are two other important parameters. The momentum coefficient allows the weight change value to be added to the next change in a certain amount in the learning process [14].

B. SUPPORT VECTOR MACHINES (SVM)

The support vector machine (SVM) is a classification technique that can be used for both linear and non-linear problems. The basic approach in SVMs is based on finding the best decision boundary that separates the two classes, namely hyperplane [15]. The SVM initially applied for linear classifications was then applied to nonlinear problems with the addition of kernel functions. Because real-time problems are largely unsuitable for linear decomposition, which makes the use of kernel functions a requirement. The data cannot be separated linearly, it is moved from one dimension to another using kernel functions, and they can be linearly separated in this new space [16].

Choosing the appropriate kernel function is very important for correct classification. The most commonly used kernel functions in the literature are polynomials, normalized polynomials, Pearson VII and radial basis kernel functions, and radial basis function (RBF) is the most successful kernel function among them. RBF is used in this study and the mathematical expression is calculated as

$$K(x,y) = e^{-\gamma|x-x_i|^2} \qquad (4)$$

Here, γ refers to the kernel dimension.

C. K-NEAREST NEIGHBORS (K-NN)

k-nearest neighbors (k-NN) is a successful classification technique that is often used to classify data in pattern recognition and machine learning areas [17]. The label value of the pattern is marked according to the k neighbor(s) which is closest to itself. If the majority of the neighbors belong to which class, the pattern to be recognized belongs to that class. The key parameter in the performance of the k-NN algorithm is to determine the best k value. One of the most commonly used methods for determining the best k value is cross-validation. Another important parameter is the distance metric used to calculate the closeness between patterns. there are studies on Euclid, Hamming, Mahalanobis, Manhattan, Minkowski, Cosine distances in the literature. As a result, the Euclidean distance was preferred in this study as it gave more positive results in the previous studies. Euclidean distance between two points is calculated as

$$d = \sqrt{(A_1 - B_1)^2 + \dots + (A_N - B_N)^2} \quad (5)$$

V. RESULTS AND DISCUSSION

In this study, RQA parameters were calculated to classify healthy and epileptic individuals. As a result, the Chi-square test was applied to determine the distinctive RQA parameters. According to this, 6 of the 8 RQA parameters were found: RR, DET, L, ENTR, LAM, TT.

For k-NN, 10-Fold Cross Validation (10-FCV) was used for the analysis of k value. The k values and the classification accuracy determined for each group are given in Table III.

Table 3. Classification accuracy of k-NN classifier

Groups	The best k value	Sensitivity (%)	Specificity (%)	Accuracy (%)
AB-E	1	100	92.8	96.4
AB-CD	3	87	85.9	86.4
AB-CDE	3	87.4	89.1	88.4
CD-E	1	91	82.2	86.6

The kernel-based SVM classifier is used to solve non-linear problems. An important parameter in the SVM classification which performed by Gauss RBF is the σ parameter representing the radial diameter. For the best σ value, 10-FCV was used as in k-NN. Classification results are given in Table IV.

Table IV. Classification accuracy of SVM classifier

Groups	The best σ value	Sensitivity (%)	Specificity (%)	Accuracy (%)
AB-E	0.7	98.4	92.4	95.4
AB-CD	0.5	87.9	83.7	85.8
AB-CDE	0.5	86	86.2	86.1
CD-E	0.3	94.2	82.6	88.4

Finally, the MLANN system is designed to consist of input layer with 6 neurons, hidden layer with 40 neurons and output layer with 1 neuron. Sigmoid activation function was used and the learning and momentum coefficients were determined as 0.2 and 0.3, respectively. The classification results obtained are given in table V.

Table V. Classification accuracy of MLANN classifier

Groups	Sensitivity (%)	Specificity (%)	Accuracy (%)
AB-E	96	89.4	92.7
AB-CD	97.8	98.08	97.05
AB-CDE	97.5	93.5	95.5
CD-E	95.7	85.5	90.6

According to this, the highest classification rate is seen in the case of using MLANN, in the non-seizure period when the patients and healthy individuals are distinguished. The most important advantage of this method is that it can be thought of as processing in time space without moving the sign to another space. However, since the creation of the RP takes a long time, when the signal size increases, the size of the RP can be reduced by performing a size reduction on the signal during the preprocessing step. Otherwise, in the previous work [18] the default values were used to generate the RP. In this study, the parameters that are effective in the creation of the RP are obtained by optimizing with the existing algorithms. As a result, it is also seen that the classification accuracy achieved in the previous study is over.

ACKNOWLEDGMENT

The study is selected from International Engineering Research Symposium-UMAS 2017 (Duzce University).

REFERENCES

[1] H. Reynolds, "Epilepsy: The Disorder," Epilepsy Atlas, pp. 15-27, 2005.
[2] "Epilepsy Foundation", received from the address: http://www.epilepsy.com/learn/epilepsy-101/what-epilepsy.
[3] G. D. Cascino, "When drugs and surgery don't work", *Epilepsia*, vol.9, pp. 79-84, 2008.
[4] R. M. Rangayyan, *Biomedical Signal Analysis*, Canada: John Wiley & Sons, Inc., 2002.
[5] R. G. Andrzejak, K. Lehnertz, F. Mormann, C. Rieke, P. David and C. E. Elger, "Indications of nonlinear deterministic and finite-dimensional structures in time series of brain electrical activity: Dependence on recording region and brain state", *Physical Review E*, vol. 64, no.6, 2001.
[6] T. Gautama, D. P. Mandic and M. M. V. Hulle., "Indications of nonlinear structures in brain electrical activity." *Physical Review E*, vol. 67, no. 4, 2003.
[7] N. Kannathal, M. L. Choo, U. R. Acharya and P. K. Sadasivan, "Entropies for detection of epilepsy in EEG", *Computer methods and programs in biomedicine*, vol. 80, no. 3, pp. 187-194, 2005.
[8] T. Tzallas, M. G. Tsipouras and D. I. Fotiadis, "Automatic seizure detection based on time-frequency analysis and artificial neural networks", *Computational Intelligence and Neuroscience*, 2007.
[9] K. Polat and S. Güneş, "Classification of epileptiform EEG using a hybrid system based on decision tree classifier and fast Fourier transform", *Applied Mathematics and Computation*, vol. 187, no. 2, pp. 1017-1026, 2007.
[10] U. R. Acharya, S. V. Sree, S. Chattopadhyay, W. Yu and P. C. A. Ang, "Application of recurrence quantification analysis for the automated identification of epileptic EEG signals", *International journal of neural systems*, vol. 21, no. 3, pp. 199-211, 2011.

[11] J. P. Eckmann, S. O. Kamphorst and D. Ruelle, “Recurrence plots of dynamical systems”, Europhysics Letters, vol.4, no.9, 973, 1987.
[12] H. Liu and R. Setiono, “Chi2: Feature selection and discretization of numeric attributes”, *Tools with artificial intelligence*, pp. 388-391, 1995.
[13] E. Alpaydın, *Yapay Öğrenme*, Boğaziçi Üniversitesi Yayınevi, İstanbul, Mart 2011.
[14] E. Öztemel, *Yapay Sinir Ağları*, Papatya Yayıncılık, İstanbul, 2006.
[15] S. Abe, *Support Vector Machines for Pattern Classification*, Springer, Newyork, 2010.
[16] C. Cortes and V. Vapnik, “Support Vector Networks”, *Machine Learning,* vol. 20, pp. 273-297, 1995.
[17] D. T. Larose, *Discovering Knowledge in Data*, A John Wiley & Sons Inc. Publication, Newyork, 2005.
[18] Kutlu and C. Kose, “Detection of epileptic seizure from EEG signals by using recurrence quantification analysis” presented at the 22nd IEEE Signal Processing and Communications Applications Conference (SIU), pp. 1387-1390, Trabzon, 2014.

BIOGRAPHIES

Funda Kutlu Onay received the BSc and MSc degrees from the Karadeniz Technical University (KTU), Computer Engineering Department, in 2011 and 2013 respectively. She is currently PhD student at the same university and research assistant in Computer Engineering Department of Amasya University. Her research interests are biomedical signal processing, pattern recognition and human-computer interfaces.

Cemal Kose received the BSc and MSc degrees from the Karadeniz Technical University, Turkey, in 1986 and 1990 respectively. He received a PhD degree from the University of Bristol, UK, in 1997. He became associate professor in 2009 and full professor in 2014 at the Karadeniz Technical University (KTU). He is currently professor in the Department of computer Engineering at KTU. His research interests are medical image processing, pattern recognition and information extraction.

THE JOURNAL OF
COGNITIVE SYSTEMS
VOLUME 02 NUMBER 01 JUNE 2017

HISTOGRAM AND FUZZY C-MEANS BASED AUTOMATIC THRESHOLD SELECTION FOR EDGE DETECTION PROCESS BASED ON RELATION MATRIX IN COLOR IMAGES

Ferzan Katircioglu[1]
[1]Duzce University, Duzce, Turkey

Borders of objects and shadows in the image, reflections and lighting changes within objects are named as edge. The image features of the pixel with itself and its neighbors, play a significant role in detection of the edges. Automatic threshold edge detection algorithms on the similarity image obtained from color images have been proposed in this study. Firstly, the relation matrix based on the similarity feature between neighbor pixels is utilized and the color image is converted into two-dimensional similarity image. In the second stage, histogram curve and fuzzy c-means method have been employed to obtain the automatic threshold value. Threshold values obtained by virtue of these two methods have been applied to similarity images obtained separately by Linear, Exponential and Gaussian functions. Visual results have been utilized for the performance evaluations of the two algorithms. Thin edges have been created in the histogram-based edge detection algorithm while distinct and thick edges have been created in the fuzzy c-means algorithm. Clear and distinct edges have been created in linear and exponential functions. The results of the other two methods have been achieved in the Gaussian function, through utilization of the low *D* coefficient. The edge detection results are within acceptable measures and have responded to high performance and have the feature of to be applicable to large image types.

Index Terms —Histogram, similarity image, relation matrix, edge detection, fuzzy C-means

I. INTRODUCTION

SHADOW boundaries, reflection and illumination changes in the image are named as edge. The oldest color edge detection applications generally consist of applications parallel to monochrome edge detectors. Robinson has studied on derivative edge detection for color images [1]. The edge operators suggested for the gray level images in the processes subsequent to this study are obtained for color images by the vectorial sums of the individual components' derivatives [2-4]. Machuca [5] and Cumani [6] have employed vector slopes and second derivative operators.

A different application in solution of the edge detection problem of color images is basing on the ordered statistics of the vectors [7]. Morphological edge detector has been inspired in this application. Applications which work in the way of integrating them is followed for determining the maximum and minimum places of the display function and for an edge pixel[8- 9].

An effective edge detector structure which is both correct, computable and learnable has been presented in image paths in fast edge detection structure which is one of the edge detection works carried out recently. A learning framed structure applied to random decision forests has been utilized within the local border mask. Fast real-time performance results are considered as the most important advantage [10]. In another study, Sobel and Interval Type-2 Fuzzy System based edge detection method has been proposed for color images. Color images are applied to this database in as much as foregoing provide more edge information compared to gray level images [11]. The edge detection operator named ACO has realized the fusion of the Hue and PCA components. Comparison with existent techniques has been made through utilization of Pratt's value parameter [12].

Similarity Image based on proposed Relation Matrix, Histogram Based and Fuzzy C-Means Based Edge Detection processes are presented in the second part of this study. In the third part, the algorithms have been applied to the image of the peppers which is commonly used in image processing applications. In the last part, evaluations are made as to the cited method and the applicable features of the edge detection operator are stated.

Manuscript received April 14, 2017; accepted May 25, 2017.
Corresponding author: Ferzan Katircioglu (E-mail: ferzankatircioglu@duzce.edu.tr; ORCID® ISNI: 0000-0001-5463-3792).
Digital Object Identifier:

II. HISTOGRAM AND FUZZY C-MEANS BASED AUTOMATIC THRESHOLD SELECTIONFOR EDGE DETECTION IN COLOR IMAGES

To realize the edge detection process in the image within the framework of the proposed method has been divided into two parts.

+ To obtain a similarity image based on the relation matrix,
+ To make the Edge Detection process based on Histogram and Fuzzy c-means on the obtained similarity image.

A. Obtaining the Similarity Image based on the Relation Matrix

The similarity image denotes the gray level image obtained by using the color properties of the pixels. First process to be performed is to applying a *3x3* mask on the image. As seen in figure 1 the pixel indicated by P_9 constitutes the center pixel of the mask [13]. By taking the center pixel as basis, the color distances with neighbors is found utilizing "Minkowski metric" in the R_n Euclidean space [14]. In (1) degree of is specified with a conventional approach while *p=1* is named as function city blocks and *p =2* is named as the Euclidean distance.

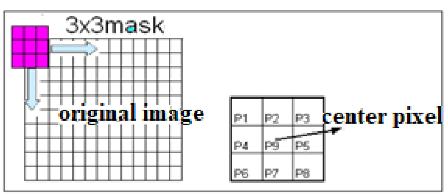

Fig. 1. Place of the mask on the image and location of the center pixel [15]

$$d = \left(\sum_{i=1}^{n} |x_i - y_i|^p \right)^{1/p} \quad (1)$$

Equation (2) is obtained if the distance between two pixels as $P_i(R_i,D_i,B_i)$ and $P_j(R_j,D_j,B_j)$ is applied to the Euclidean distance which is one of the distance methods provided here in above.

$$d_{ij} = \frac{1}{\sqrt{3}} \sqrt{(R_i - R_j)^2 + (G_i - G_j)^2 + (B_i - B_j)^2} \quad (2)$$

The distance approach provided in (2) is applied to the general functions given below and the similarity measurement between all the pixels in the mask are found [15].

$$S(i,j) = 1 - \frac{d_{ij}}{D} \quad (3)$$

$$S(i,j) = \exp\left(\frac{-d_{ij}^{\ 2}}{D^2}\right) \quad (4)$$

$$S(i,j) = \exp\left(\frac{-d_{ij}^{\ 2}}{D^2}\right) \quad (5)$$

The *D* coefficient in (3), (4) and (5) has been named as the normalization coefficient, and ensures the realization of the similarity value in the range of [0 and 1].

$$\begin{bmatrix} S(1,1) & S(1,2) & . & . & . & S(1,9) \\ S(2,1) & S(2,2) & . & . & . & S(2,9) \\ . & . & . & . & . & . \\ . & . & . & . & . & . \\ . & . & . & . & . & . \\ S(9,1) & S(9,2) & . & . & . & S(9,9) \end{bmatrix} \quad (6)$$

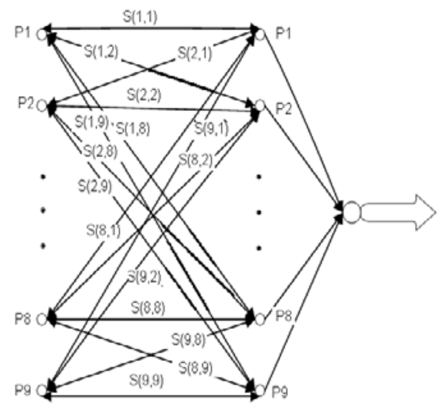

Fig. 2. The similarity network of the pixels in the mask

A mask under the relation matrix is shown in figure 2 while in (6) the similarity value which will be in the similarity image is calculated [15].

$$S_{merkez} = \frac{1}{81} * \sum_{i=1}^{9} \sum_{j=1}^{9} S_{ij} \quad (7)$$

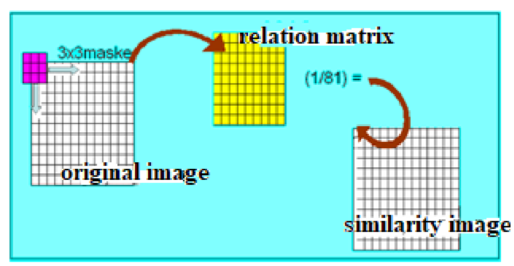

Fig. 3. Obtaining the similarity image [15]

As shown in figure 3, *3x3* mask has been applied on the real image and similarity values have been found by using distance finding between pixel method for the center pixel. *9x9* similarity relation matrix is created for the center pixel, the average value is found and recorded to the relevant pixel value [17].

B. Edge Detection of Automatic Threshold by Histogram Curve

Histogram of an image with [0, L-1] gray level interval is a discrete function and image statistic method gives the pixel number gray level values [18]. The histogram of the similarity image is first obtained in the flow pseudo code of which is provided in algorithm 1. Two peak points are searched in the histogram curve as the third step. One of the most important points here is to pay attention to the degree of proximity between the cited peak points. The threshold value is obtained by taking the average of the gray level values of the two obtained peak points.

$$S_{T,k} = \frac{L(Pik1) + L(Pik2)}{2} \tag{8}$$

Alg. 1. Pseudocode for automatic threshold edge detection by using histogram

Step 1. *Obtain similarity image*
Step 2. *Obtain the histogram of the similarity image*
Step 3. *Find two large peak values on the histogram*

$$\mathbf{S_{T,k}} = \frac{\mathbf{L(Pik1)+L(Pik2)}}{\mathbf{2}}$$

Step 4. *Do Edge Dedection*
if $S_{ij} > S_{T,k}$ **then** ***isnt edge.***
if $S_{ij} \le S_{T,k}$ **then** ***is edge.***

Finally, each pixel of the similarity image has been passed through the $S_{T,k}$ threshold by using the criterion in (9).

$$\begin{aligned} &\text{If } S_{ij} > S_{T,k} \text{ than the pixel isn't edge} \\ &\text{If } S_{ij} \le S_{T,k} \text{ than the pixel is edge} \end{aligned} \tag{9}$$

If S_{ij} is smaller than $S_{T,k}$ value it means that it is not similar with its environment. Not being similar, or in other words the existence of sharp changes reveals the edge property.

C. Edge Detection of Automatic Threshold by Fuzzy C-Means

FCM(Fuzzy c-means algorithm) found by Bezdek and after improved by many different approaches is one of the most popular fuzzy clustering algorithms [19]. The fuzzy c-means algorithm works to minimize the objective function, which is the generalization of the method of least squares.

$$Jm = \sum_{i=1}^{N}\sum_{j=1}^{C} u_{ij}^{m}\|X_i - C_j\|^2 \qquad 1 \le m < \infty \tag{10}$$

In u_{ij}^{m} in (10) "i" represents the object while "j" represents its membership value of the cluster. $1 \le m < \infty$ value is expressed as fuzziness degree or fuzziness agent in fuzzy clustering algorithm.

In $\|X_i - C_j\|^2$ "i" represents the object and "j" represents the distance between it and the cluster center, and the Euclidean distance is used. Clustering centers are calculated after the membership values are randomly assigned. Cluster centers are detected according to the (11) below.

$$C_j = \sum_{i=1}^{N} u_{ij}^{m} X_i \Big/ \sum_{i=1}^{N} u_{ij}^{m} \tag{11}$$

The membership value in (12) is compared with the old value from the previous cycle. The process continues until comparison is less than the minimum value ε [20].

$$u_{ij} = \frac{1}{\sum_{k=1}^{C}\left(\frac{\|X_i - C_i\|}{\|X_i - C_k\|}\right)^{2/(m-1)}} \tag{12}$$

Alg. 2. Pseudocode for automatic detection of automatic threshold edge by using FCM

Step 1. *Obtain similarity image*
Step 2. *Run Fuzzy C- Means (FCM)*
Number of clusters = 2; m = 2;
ε = 0.001; iteration = 20;
Find C1 ve C2
Step 3. *Calculate threshold value*

$$\boldsymbol{S_{T,k}} = \frac{\boldsymbol{C1+C2}}{\boldsymbol{2}}$$

Step 4. *Do Edge Dedection*
if $S_{ij} > S_{T,k}$ **then** ***isnt edge.***
if $S_{ij} \le S_{T,k}$ **then** ***is edge.***

The fuzzy c-means clustering method specified briefly hereinabove has been utilized to separate the similarity image into two separate clusters in the presented study. The average of the centers of two clusters gives the threshold value for edge detection according to the flow provided in algorithm 2.

III. DISCUSSION

Fig. 4. Pepper image which is widely used in literature

The very well-known pepper picture seen in figure 4 has been utilized for image processing for the method used. It is a color image with the size of 256x256. The presented work has been applied in Matlab R 2012b version of the computer with features of Intel (R) Core (TM) i5-4200U CPU 1.60 GHz 2.30 GHz processor, 6 GB RAM and 64 bit Operating System. An interface has been designed in Matlab Gui for Edge Detection process. Firstly *D* value and the function it will work with it is determined in the interface design seen in figure 5 named Edge Detection. Histogram or fuzzy c-means based automatic edge detection process is made on the obtained similarity image depending on the user's wish.

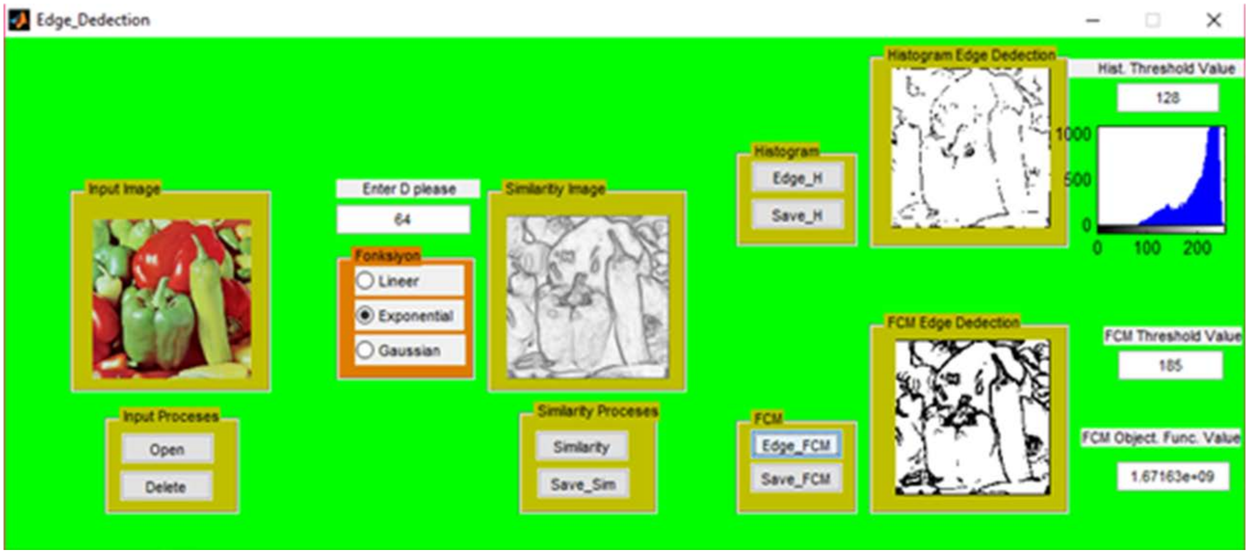

Fig. 5. Edge_Detection interface design

D normalization coefficient value, used to obtain the similarity image, has been selected as 64 for all applications. The thin edges have been created in the histogram-based edge detection algorithm in figure 6. (a), (b) and (c), while distinct and thick edges have been created in the fuzzy c-means algorithm in figure 6 (d), (e) and (f). Fuzzy C-means method is remarkable in achieving the edges, formation of different threshold values, and distinctness of the edges.

Contamination of the similarity image in figure 6 (a) and (d) linear function has been removed in both methods. The most important feature of the exponential function in figure 6 (b) and (e) is that as the distance between pixels becomes larger, the percentage of reduction rate of the similarity takes place with bigger changes. As such, contamination has been reduced and more flattened image has been obtained. The similarity output characteristic of equality in (5) is similar to exponential function. Glossy and clear images were obtained when figure 6 (c) and (f) has been analyzed. However, the disappearance of the image edges, even to a small extent, has occurred.

IV. CONCLUSIONS

The most important feature of the method used is that the color information in the color image is reduced by a one-dimensional smoothing process. Clean and well-defined edges have been formed in the linear and exponential function. If the

EDGE DETECTION OF AUTOMATIC THRESHOLD BY HISTOGRAM CURVE			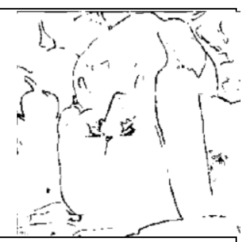
	(a) $S_{T,k}$ =128 Eq. (3)	(b) $S_{T,k}$ =128 Eq. (4)	(c) $S_{T,k}$ =128 Eq. (5)
EDGE DETECTION OF AUTOMATIC THRESHOLD BY FUZZY C-MEANS			
	(d) $S_{T,k}$ =129 Eq. (3)	(e) $S_{T,k}$ =185 Eq. (4)	(f) $S_{T,k}$ =194 Eq. (5)

Figure 6. Automatic edge detection threshold images with histogram curve and fuzzy c-means

edges are thick and there is a contaminated environment, *D* value is increased and finer images can be achieved and if the edges are obscure, *D* value is increased and the correction operation can be done. Selection of high threshold value can be achieved by the use of low *D* coefficient in the Gaussian function. The thin edges have been created in the histogram-based edge detection algorithm while distinct and thick edges have been created in the fuzzy c-means algorithm. The results of edge detection are within acceptable measures and have responded at high performance. They can be applied to wide image types. Furthermore, it is aimed to use the edge detection process via similarity image also in works for image correction and compression by evaluating the feature information again in the original image.

ACKNOWLEDGMENT

The study is selected from International Engineering Research Symposium-UMAS 2017 (Duzce University).

REFERENCES

[1] Robinson, G.S., Color edge detection, Opt. Eng., vol. 16, no.5, pp. 479-484, Sep/Oct. 1977.

[2] Rosenfeld, A., and Kak, A.C., Digital Picture Processing, New York: Academic, 2d ed., 1982.

[3] Shiozaki, A., Edge extraction using entropy operator, *Comp. Vis. Graph. Image Proc.,* vol. 36, pp. 1-9, 1986.

[4] Zenzo, S.D., A note on the gradient of a multiimage, *Comp. Vis. Graph. Image Proc.,* vol. 33, pp. 116-125, 1986.

[5] Machuca, R., and Phillips, K., Applications of vector fields to image processing, *IEEE Trans. Pattern Anal. Machine Intel.,* vol. PAMI-5, no.3, pp. 316-329, May 1983.

[6] Cumani, A., Edge detection in multispectral images, *CVGIP: Graphical Models and Image Processing,* vol. 53, no. 1, pp. 40-51, Jan. 1991.

[7] Barnett, V., The ordering of multivariate data, *J. Royal Statist. Soc. A*, 139, pt. 3, pp. 318-343, 1976.

[8] Feechs, R.J. and Arce, G.R., Multidimensional morphologic edge detection, *In Proc. SPIE Conf. Visual Comm. and Image Proc*., vol. 845, pp. 285-292, 1987.

[9] Lee, J.S.J., Haralick, R.M., and Shapiro, L.G., Morphologic edge detection , *IEEE J. Robot. Automat*., vol. RA-3, no.2, pp. 142-156, Apr. 1987.

[10] Dollár, P., & Zitnick, C. L. Fast edge detection using structured forests. *IEEE transactions on pattern analysis and machine intelligence,* 37(8), 1558-1570, 2015.

[11] Melin, P., Gonzalez, C. I., Castro, J. R., Mendoza, O., & Castillo, O. Edge-detection method for image processing based on generalized type-2 fuzzy logic. *IEEE Transactions on Fuzzy Systems,* 22(6), 1515-1525, 2014.

[12] Sharma, K., & Chopra, V. ACO Based Color Edge Detection on the Fusion of HUA and PCA Components. *International Journal*, 5(6), 2015.

[13] Demirci, R., "Rule-based automatic segmentation of color images",*International Journal of Electronics and Communications(AEU)*,60,435-442, 2006.

[14] Trahanias, P.E., Venetsanopoulos, A.N., "Vektör Order Statistics Operators as Color Edge Detectors", *IEEE Tran. On Systems, Man and Cybernetics-Part B Cybernetics,* Vol 26 No1 , 1996.

[15] Katircioglu, F., "Segmentation of color images based on relation matrix and edge detection", Master of Science, Dept. Electrical Education, Duzce Universtiy, Duzce, Turkey 2007.

[16] Demirci, R. Similarity relation matrix-based color edge detection. AEU-international journal of electronics and communications, 61(7), 469-477, 2007.

[17] Demirci, R., Katircioglu, Segmentation of color images based on relation matrix. *Signal Processing and Communications Applications,* SIU 2007. IEEE 15th, 2007.

[18] Rafael C. Gonzalez ve Richard E. Woods, Sayısal Gö- rüntü ˙I¸sleme (3. Baskı), Palme Yayıncılık, 2014.

[19] Bezdek, J. C., Ehrlich, R., & Full, W. (1984). FCM: The fuzzy c-means clustering algorithm. *Computers & Geosciences*, 10(2-3), 191-203.

[20] Moertini, V.S.: "*Introduction To Five Clustering Algorithms*", Integral, Vol. 7, No. 2, 2002.

BIOGRAPHIES

Ferzan Katircioglu was born in Turkey. He received B.Sc. in 1996 at Marmara University, Faculty for Technical Education, M.Sc. in 2007 at A.I.B.U., Institute for Natural Sciences, Department of Electricity Education and Ph.D. at Düzce University, Faculty for Natural Sciences, Department of Electricity-Electronis and Computer Engineering in 2016. He has worked as academic staff in the Control and Automation Technolpogy program at Düzce University, Düzce Vocational High School since 2000. His current research interests are Imagel Processing and Heuristic Optimization.

THE JOURNAL OF
COGNITIVE SYSTEMS
VOLUME 02 NUMBER 01 JUNE 2017

PREDICTION OF SOLAR RADIATION BASED ON MACHINE LEARNING METHODS

Seckin Karasu[1], Aytac Altan[1], Zehra Sarac[1], Rifat Hacioglu[1]
[1]Bülent Ecevit University, Zonguldak, Turkey

In this study, machine learning methods which linear regression and Gaussian process regression models are used to estimate the solar radiation on daily data set taken from the wind central in Zonguldak province in Turkey. The measured wind speed, temperature, pressure, humidity parameters together with solar radiation are used for the prediction process. In the prediction process, number of delay steps from 3 to 12 for these parameters are applied to the developed models. In order to determine the performance of the obtained model, the model is evaluated in terms of statistical error criteria such as MAE, MSE and RMSE. The least prediction error for the solar radiation prediction process is determined. It has been observed that Gaussian regression model approach provides a high performance to predict solar radiation with related to other measured parameters.

Index Terms—Solar radiation, prediction, linear regression, Gaussian process regression, machine learning

I. INTRODUCTION

MACHINE learning models are used to find a relationship in pattern recognition and classification problems where there is no representation between input and output, in data mining and prediction problems [1]. In machine learning models, there are supervised learning methods such as linear regression, nonlinear regression, artificial neural networks [2, 3], support vector machine, k-nearest neighbors. Beside them, there are unsupervised learning methods and ensemble learning methods [1].

In the literature, single and hybrid estimator models are constructed for the estimation of hourly solar radiation. In the first stage, Multi-Layer Perception (MLP), Autoregressive Moving Average (ARMA) and persistence models are established. In the second stage, these are combined with Bayesian rules, resulting in a 14% improvement in the estimate [4]. Polynomial Basis Function (PBF) and Radial Basis Function (RBF) based Support Vector Regression (SVR) method are used for daily solar radiation estimation. It is shown that the SVR method based on PBF with different statistical indicators has higher prediction performance for 1460 days solar radiation data [5]. Support Vector Machine (SVM) and Wavelet Transform (WT) methods have been combined to develop a hybrid estimation method. The proposed method is compared with other methods such as Artificial Neural Network (ANN), Genetic Programming (GP) and ARMA. It has been shown that the proposed prediction model gives a low error value in estimating the solar radiation for the different input parameters [6]. Genetic Algorithm (GA) and pruning method based on optimal NARX estimator based on optimal brain surgeon optimization methods are used for wind speed and solar radiation estimation. The wind speed and solar radiation are estimated for different time periods from 8 hours to 24 hours. It is mentioned that the proposed method can be applied in photovoltaic (PV) estimation and wind power generation [7]. In [8], monthly temperature, sunshine duration, meteorological data are used for solar radiation estimation. Adaptive Neuro-Fuzzy Inference System (ANFIS) is used in the estimation phase. It is stated that the proposed model is effective for practical applications.

In this study, solar radiation estimation is done by linear regression and Gaussian process regression methods using 1-year data consisting of daily time series. For wind speed, temperature, humidity and pressure variables, the coefficients obtained by the 1st order curve fitting method are calculated attached to the number of delay steps and are applied to the models. In the phase of model training, 10-fold cross-validation method is used. According to the model results, models created with statistical indicators such as MAE, MSE and RMSE are calculated for different delay step counts. It is seen that the minimum MSE value for estimating the solar radiation value is given by the Gaussian Process Regression model for delay step count 11.

This article is organized as follows: used methods and modelling are presented in Section II. Simulation and experimental results are given in Section III. Conclusions are finally discussed in Section IV.

II. USED METHODS AND MODELLING

In this study, one-year data consisting of daily data taken from meteorological station in Zonguldak province is used for solar radiation estimation. The maximum, minimum, mean and standard deviation values for wind speed, temperature, relative humidity, current pressure and solar radiation variables in the used data set are given in Table I. For solar radiation, hourly data values are summed to get daily data set.

Manuscript received April 20, 2017; accepted May 25, 2017.
Corresponding author: Rifat Hacioglu (E-mail: hacirif@beun.edu.tr; ORCID® ISNI: 0000-0002-2480-0729).
Digital Object Identifier:

Table I. Statistical Values of Variables

Parameters	Max.	Min.	Mean	Std. Dev.
Wind Speed (m/s)	5	0	2.07	0.78
Temperature (°C)	26.2	0.2	15.03	7.17
Humidity (gr/m3)	99	31	75.66	14.40
Pressure (mbar)	1016	978	999	6.13
Solar radiation (W/m2)	22130	480	10864	6382

A. Multiple Linear Regression Model

A In the multiple linear regression model, the relationship between multiple independent variables ($x_1,\ x_2,\ x_3,\ x_4$) and a dependent variable ($\hat{y}$) is examined. The regression function used in this study is the first order, and it is assumed that each independent variable is a linear relationship with the dependent variable, as in (1)

$$\hat{y} = b_0 + b_1 x_1 + b_2 x_2 + b_3 x_3 + b_4 x_4 \quad (1)$$

where b_0 is the y-axis cut point of the modified regression curve, b_1 is the coefficient x_1 of the first guess variable, and b_2 is the coefficient x_2 of the first guess variable so on.

In this study, wind speed, temperature, humidity, pressure are used as independent variable ($x_1,\ x_2,\ x_3$ and x_4) respectively and solar radiation is used as a dependent variable ($\hat{y}$).

B. Gaussian Process Regression Model

In supervised learning, it is expected that similar predictor values x_i and response values y_i have close. In Gaussian processes this similarity is given by a related covariance function [9]. It is determined the covariance between two latent variables $f(x_i)$ and $f(x_j)$ for $i \neq j$. The signal length of the predictor is expressed as N.

The covariance function is expressed by different kernel functions such as Squared exponential, Exponential, Gibbs, Matérn and Rational quadratic kernel. The rational quadratic kernel is used in this study. The covariance function $k(x_i, x_j)$ can be expressed as $k(x_i, x_j|\hat{y})$ in (2) in terms of kernel parameters in the $\hat{y}$ vector.

$$k\left(x_i, x_j \mid \hat{y}\right) = \sigma_f^2 \left(1 + \frac{r^2}{2\alpha\sigma_l^2}\right)^{-\alpha} \quad (2)$$

$$r = \sqrt{\left(x_i - x_j\right)^T \left(x_i - x_j\right)} \quad (3)$$

σ_f and σ_l denote the signal standard deviation and characteristic length scale, respectively. α indicates rational quadratic exponent. The value of r in (3) is the Euclidean distance between x_i and x_j. It is possible to use a separate length scale (σ_m) for each predictor $m,\ m = 1, 2, \dots, N$. For each predictor, covariance functions with separate length scale implement automatic relevance determination (ARD). In this case, the covariance function, $k(x_i, x_j|\hat{y})$ is expressed as in (4).

$$k\left(x_i, x_j \mid \hat{y}\right) = \sigma_f^2 \left(1 + \frac{1}{2\alpha} \sum_{m=1}^{N} \frac{\left(x_{im} - x_{jm}\right)}{\sigma_m^2}\right)^{-\alpha} \quad (4)$$

C. Feature Extraction and Normalization with Curve Fitting

Using (5), coefficients of curve fitting in the first order linear function are calculated taking into account the number of delay steps for wind speed, temperature, humidity and pressure values.

$$\hat{y} = \varphi_i x + \psi_i \quad (5)$$

Table II. Extracted Features and Their Labels

Parameters	Features	Feature label
Wind Speed	$[\varphi_1, \psi_1]$	F1 F2
Temperature	$[\varphi_2, \psi_2]$	F3 F4
Humidity	$[\varphi_3, \psi_3]$	F5 F6
Pressure	$[\varphi_4, \psi_4]$	F7 F8

The min-max normalization equation in (6) is used for the feature coefficients in Table II and solar radiation variable.

$$f_{i,new} = \frac{f_{i,old} - f_{min}}{f_{max} - f_{min}} \quad (6)$$

where f is the feature vector, f_i is i th element of feature vector, $f_{i,old}$ is the old value of i th element in feature vector, f_{max} is the maximum value of feature vector, f_{min} is the minimum value of feature vector, $f_{i,new}$ is the new value of i th element in feature vector. In Table I, the range values for all variables are converted to the range $[0, 1]$.

D. Evaluation of Model Accuracy

There is no single criterion for evaluating the performance of the model. Graphical representations can give an idea of model performance. Model performance can obtained by plotting the estimated time series on the real time series. Distribution of the error can be observed with the scatter plot [1].

Apart from these, there are indicators that represent mathematical model performance. In Equation (7-9), Mean Absolute Error (MAE), Mean Squared Error (MSE) and Root Mean Squared Error (RMSE) are given.

$$MAE = \frac{1}{N} \sum_{n=1}^{N} \left|e_n\right| \quad (7)$$

$$MSE = \frac{1}{N} \sum_{n=1}^{N} e_n^2 \quad (8)$$

$$RMSE = \sqrt{\frac{1}{N}\sum_{n=1}^{N} e_n^2} \quad (9)$$

The error is expressed

$$e_n = y_n - \hat{y}_n \quad (10)$$

where y_n is observed for a given time n and $\hat{y}_n$ is the predicted time series. The Pearson linear correlation coefficient, which is an indicator of the relationship between input and output for $m = 4$, is calculated as

$$R = \frac{\sum_{i=1}^{m}(x_i - \bar{x})(y_i - \bar{y})}{\sqrt{\sum_{i=1}^{m}(x_i - \bar{x})^2}\sqrt{\sum_{i=1}^{m}(y_i - \bar{y})^2}} \quad (11)$$

when the R value is 1, it is said that there is a linear relationship. When the R value is 0, there is a nonlinear relationship between input and output.

III. SIMULATION AND EXPERIMENTAL RESULTS

The one-year wind speed, temperature, relative humidity, current pressure and solar radiation data from the daily time series from the meteorological station are filtered by 10-day average filter in the smoothing process. The curve fitting coefficients are obtained from each feature by the first order curve fitting method. In this study, solar radiation estimation is performed by using different numbers of delay steps for linear regression and Gaussian process regression models such as wind speed, temperature, relative humidity and current pressure values as input, solar radiation value as output.

The generated models are compared with graphical representations, error indicators and the best prediction model is chosen for number of delay steps from 3 to 12. The simulation is performed in MATLAB. The errors that occur for two different estimation models are given in Figure 1-3.

When the MAE, MSE and RMSE values are examined, it is observed that the error values decrease when the number of delay steps is increased. In the Gaussian process regression method, it is seen that the error amount is less than the linear regression method. The minimum MSE value is obtained for the Gaussian process regression model when the number of delay step is 11.

The solar radiation value estimated by the model obtained by the Gaussian Process Regression Method and the actual value are shown in Figure 4. When the estimated values of the obtained model are examined, it is seen that the error amount is very low. The relationship between the actual values and the predicted values is shown in scatter plot in Figure 5. This relation is expressed by first order linear regression with $y = 0.99x + 0.0033$ equation. R is calculated as 0.99792, and it is concluded that the model is successful in predicting the actual solar radiation values.

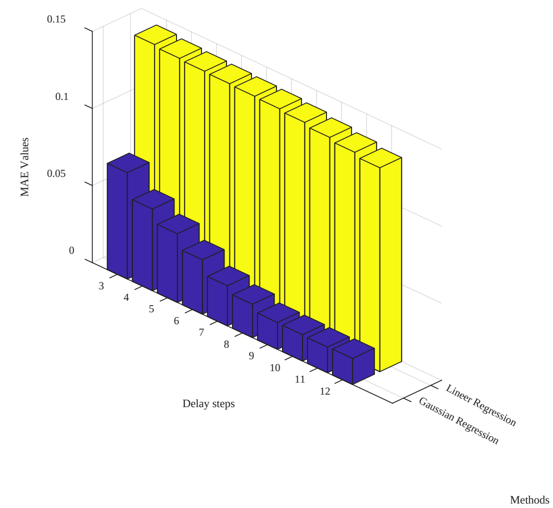

Fig. 1. The MAE change due to the number of delay steps for the two estimation methods.

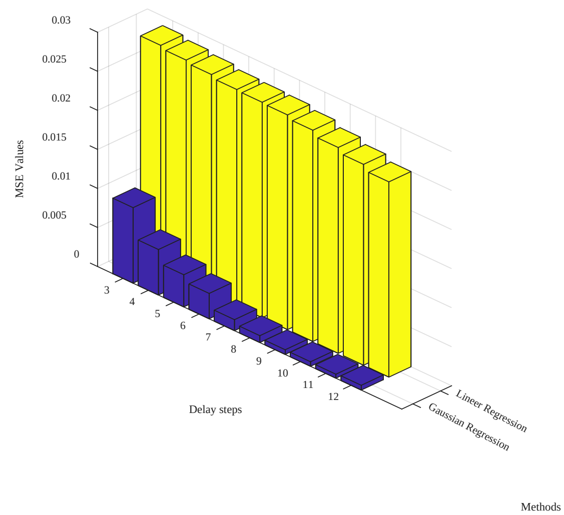

Fig. 2. The MSE change due to the number of delay steps for the two estimation methods.

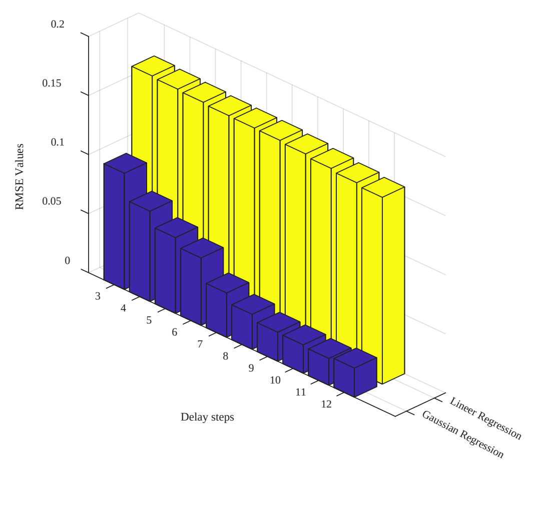

Fig. 3. The RMSE change due to the number of delay steps for the two estimation methods.

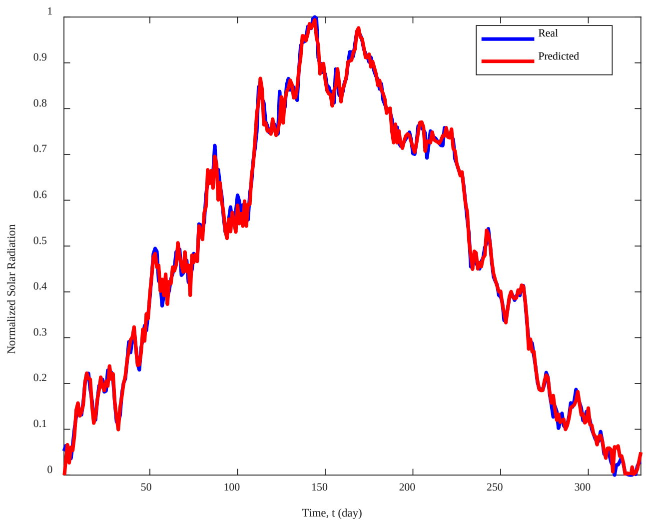

Fig. 4. Solar radiation prediction by Gaussian process regression method.

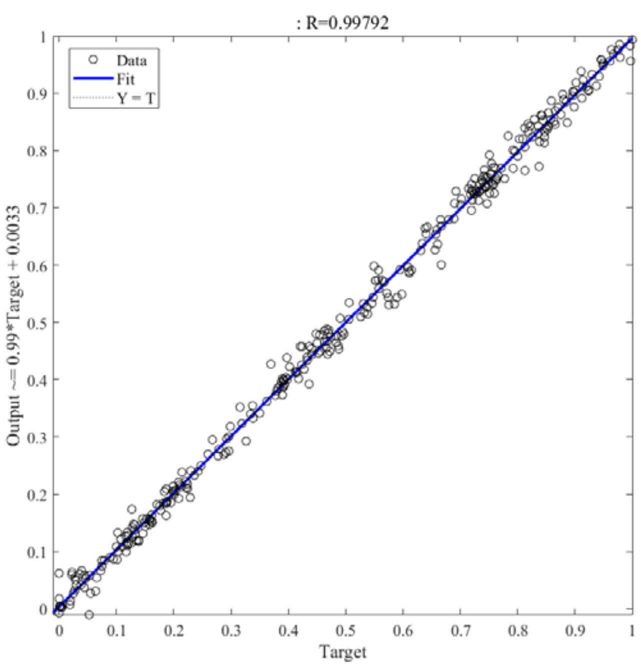

Fig. 5. Scatter plot for real and predicted points.

IV. CONCLUSIONS

In this article, linear regression and Gaussian process regression methods are used to develop a solar radiation prediction model that gives the least error. One-year wind speed, temperature, pressure, humidity and solar radiation values data consisting of one daily time series taken from meteorological station in Zonguldak province are used for solar radiation estimation. Coefficients are generated by first order curve fitting for variables outside the solar radiation. In the solar radiation prediction process, number of delay steps from 3 to 12 for these parameters are applied to the created models. In training phase, in order to measure the model performance, a 10-fold cross-validation method is applied independently of the data. It is determined that the Gaussian process regression method has a lower MSE value than the linear regression method. For the model and model parameters for which the best result is obtained, the MAE value is calculated as 0.016620, the MSE value is 0.000514 and the RMSE value is 0.022674. The predicted solar radiation versus real solar radiation for the given minimum error model is plotted. Also, it is observed that the performance is high by scatter plot.

ACKNOWLEDGMENT

This study was supported by Bülent Ecevit University (BAP Project No: 2012-17-15-01 and 2014-75737790-01). The authors would like to thank Bülent Ecevit University for their support. The study is selected from International Engineering Research Symposium-UMAS 2017 (Duzce University).

REFERENCES

[1] C. Voyant, G. Notton, S. Kalogirou, M.L. Nivet, C. Paoli, F. Motte, and A. Fouilloy, "Machine learning methods for solar radiation forecasting: A review", Renewable Energy, 105, 2017, pp. 569-582.

[2] S. Karasu, A. Altan, Z. Saraç, and R. Hacıoğlu, "Prediction of wind speed with non-linear autoregressive (NAR) neural networks", IEEE 25th Signal Processing and Communications Applications Conference, 2017, pp. 1-4.

[3] S. Karasu, A. Altan, Z. Saraç, and R. Hacıoğlu, "Estimation of fast varied wind speed based on NARX neural network by using curve fitting", International Conference on Advanced Technology & Sciences (ICAT'17), 2017, pp. 551-557.

[4] C. Voyant, C. Darras, M. Muselli, C. Paoli, M.L. Nivet, and P. Poggi, "Bayesian rules and stochastic models for high accuracy prediction of solar radiation", Applied Energy, 114, 2014, pp. 218-226.

[5] K. Mohammadi, S. Shamshirband, M.H. Anisi, K.A. Alam, and D. Petkovic, "Support vector regression based prediction of global solar radiation on a horizontal surface", Energy Conversion and Management, 91, 2015, pp .433-441.

[6] K. Mohammadi, S. Shamshirband, C.W. Tong, M. Arif, D. Petkovic, and S. Ch, "A new hybrid support vector machine–wavelet transform approach for estimation of horizontal global solar radiation", Energy Conversion and Management, 92, 2015, pp. 162-171.

[7 A. Di Piazza, M.C. Di Piazza, and G. Vitale, "Solar and wind forecasting by NARX neural networks", Renewable Energy and Environmental Sustainability, 39, 2016, pp. 1-5.

[8] L. Olatomiwa, S. Mekhilef, S. Shamshirband, and D. Petkovic, "Adaptive neuro-fuzzy approach for solar radiation prediction in Nigeria", Renewable and Sustainable Energy Reviews, 51, 2015, pp. 1784-1791.

[9] C.E. Rasmussen and C.K.I. Williams, "Gaussian processes for machine learning", MIT Press, 2006.

[10] A.G. Wilson, "Covariance kernels for fast automatic pattern discovery and extrapolation with Gaussian processes", University of Cambridge, 2014.

[11] R.M. Neal, "Bayesian Learning for Neural Networks", Toronto University Doctorate Thesis, 1995, p. 118.

BIOGRAPHIES

Seçkin Karasu is a research assistant at the Department of Electrical Electronics Engineering, Bülent Ecevit University in Turkey. He recieved the BSc and M.Sc. degrees in the department of Electrical Electronics Engineering from Bülent Ecevit University in 2011 and 2013, respectively. He is a Ph.D. candidate. His research interests are signal processing, image processing, machine learning and power systems.

Aytaç Altan is a lecturer at the Department of Electrical Electronics Engineering, Bülent Ecevit University in Turkey. He received the BSc and M.Sc. degrees in the department of Electrical Electronics Engineering from Anadolu University in 2011 and 2016, respectively. He is a Ph.D. candidate. His research interests are signal processing, machine learning, robotic systems, adaptive control and system identification.

Zehra Saraç is a Professor at the Department of Electrical Electronics Engineering at the Bülent Ecevit University in Turkey. She received the M.Sc. and Ph.D. degrees in the department of Electronics Engineering from Gebze Technical University 1996 and 2002, respectively. Her research interests are electromagnetic waves, signal processing, image processing, opto-electronics, holography, interferometry and microwave photonics.

Rıfat Hacıoğlu is an Assistant Professor at the Department of Electrical Electronics Engineering at the Bülent Ecevit University in Turkey. He received the M.Sc. and Ph.D. degrees in the department of Electrical Electronics Engineering from Illinois Institute of Technology in 1996 and 2002, respectively. His research interests are signal processing, control applications, linear and nonlinear system identification, parametric model estimation approaches, microprocessor based control systems, image identification problems.

THE JOURNAL OF COGNITIVE SYSTEMS
VOLUME 02 NUMBER 01 JUNE 2017

ESTABLISHMENT OF DIAGNOSING FAULTS AND MONITORING SYSTEM WITH NEURAL NETWORKS IN AIR CONDITIONING SYSTEMS

Hüseyin Yüce[1], Köksal Avci[1]

[1]Marmara University, Istanbul, Turkey

Despite the fact that the world has different climate regions, humankind finds a living environment in a certain temperature, humidity range and clean weather conditions suitable for him. This living environment is defined as "Comfort Zone". Today, people spend most of their daily lives in closed environments. The use of air conditioners is becoming increasingly widespread in order to create a comfortable environment in the living areas, especially shopping centers. In this study; a malfunction in an air condition was detected and the malfunction information was taken and sent to a remote server database via mobile internet infrastructure. The data on the server was processed with artificial intelligence and a mobile application was developed. Again, with an Android device with network access, it was aimed to retrieve the data from the database and forward it to the technical service personnel. An electronic card is designed for the retrieval of the fault data.

Index Terms — Fault detection and diagnosis, neural networks, mobile programing

I. INTRODUCTION

THE environments in which the air conditioner is used contribute to the increase in the work force efficiency with a healthy life. For this reason, nowadays, the air conditioner has become a necessity for human life without being luxurious. Along with an increase in demand for better living standards, today, the number of air conditioning used in the world is about 140 million and the Figure spent on them is 90 billion euros[1]. The need for the establishment of climate systems is directly linked to the development of human living standards and the resulting physiological needs[2]. Therefore, it is an important issue to intervene the malfunctioning air conditioner in the shortest time when the air conditioning systems used in every life of the life, particularly in the health sector, are malfunctioning. Especially in air conditioning systems, when faults occur simultaneously, it is often hard to differentiate those issues from one another[3].

Fault detection and diagnosis is an important problem in process engineering. Early detection and diagnosis of process faults, while the plant is still operating in a controllable region, can help avoid abnormal event progression and reduce productivity loss[4]. Although fault detection and diagnosis FDD has been an active area of research in other fields for more than a decade, applications for heating, ventilating, air conditioning, and refrigeration (HVAC&R) and other building systems have lagged those in other industries. Nonetheless, over the last decade, there has been considerable research and development targeted toward developing FDD methods for HVAC&R equipment[5]. Many models and studies have been developed and done to identify fault diagnostic errors. According to V. Venkatasubramanian et al., causal origins have to be diagnosed and identified in order to detect an abnormal event in a timely manner, and that appropriate audit control decisions and actions must be taken in order to bring it to a safe and working state and have worked on a model. In this model, diagnostic methods are divided into three general categories and examined in three parts. Quantitative and model based methods, qualitative and model based methods and process history based methods. They have prepared the model in Figure 1 for this[4].

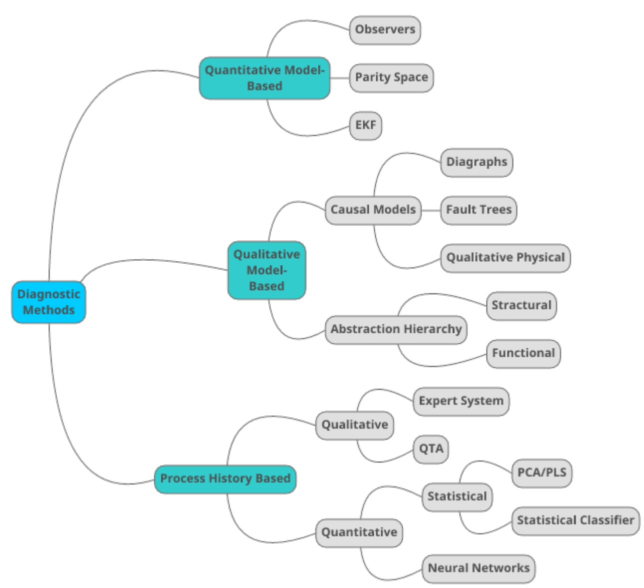

Fig. 1. Classification of diagnostic algorithms

Manuscript received April 27, 2017; accepted May 25, 2017.
Corresponding author: Hüseyin Yüce (E-mail: huseyin@marmara.edu.tr; ORCID® ISNI: 0000-0001-5525-7733).
Digital Object Identifier:

Y. Yu et al., provide a systematic review of existing fault detection and diagnosis (FDD) methods for an air-handling unit (AHU) and in reality, they introduced new approaches to high performance. For this goal, the background of AHU systems, general FDD framework and typical faults in AHUs, is described. Ten desirable characteristics used in a review of FDD in chemical process control are introduced to evaluate the methodologies and results. A new categorization method is proposed to better interpret the different and most recent approaches[6].

Basic building blocks of FDD systems, methods used to detect errors and then diagnose the causes. Several different methods are used to detect and diagnose faults. The major difference in these approaches is the knowledge used for formulating the diagnostics.

Model-based methods can use quantitative or qualitative models. Quantitative models are sets of quantitative mathematical relationships based on the underlying physics of the processes. Qualitative models are models consisting of qualitative relationships derived from knowledge of the underlying physics. The boundary between quantitative models and qualitative models can become blurred for some approaches, but this distinction and that between model-based and process history (data) based methods provide a useful scheme for categorizing FDD methods, which is used in this paper (Figure 2)[5].

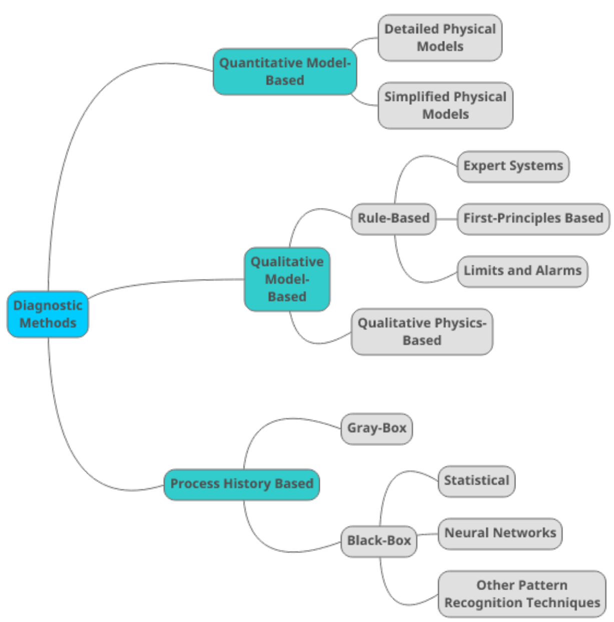

Fig. 2. Classification scheme for FDD methods

Generally, the model-based methods have been most widely developed in the HVAC systems. The good application of the model-based FDD method relies on the accurate mathematical physical models[7].

Wang et al., developed a detection model-based on a neural network in the variable air volume systems. The neural network can be used to diagnose the faults of outdoor air, supply air and return air flow rate sensors after training using operation data[8].

These studies show that neural networks are one of the most used models for fault detection and diagnosis.

In this study, It was aimed to determine the faults in an air condition and to send and process this information to a remote server via the mobile network infrastructure. For this purpose, an electronic card was designed and the air conditioner data was taken and wirelessly sent to a remote server. On the server side, a neural network model was used to classify the fault diagnosis. A mobile software has been developed for transferring online data to technical service personnel. In this way, changes and failures in the climate can be monitored in real time.

II. SYSTEM DESCRIPTION

The method used in the study consists of four stages, so the study text is given under four headings. (Figure 3). The first stage of the work is the "Air conditioning module". It consists of a simulator system that can generate the fault. The second stage which of the work is the "Microcontroller module" which is taken the data from the "Air conditioning module". The third stage is the "Server module" where the data is collected and processed. In the last stage, "User module" has been completed with the developed mobile program.

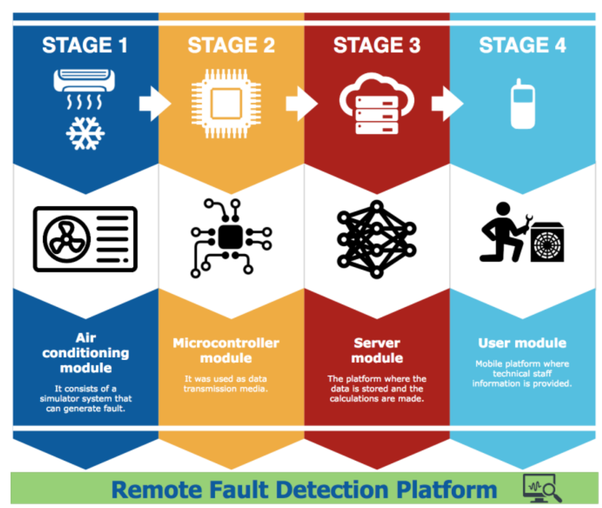

Fig. 3. Model of remote fault detection platform

A. STAGE ONE: AIR CONDITIONING MODULE

This module consists of a training simulator system in which a fault can be generated in a wall-mounted air conditioner (Figure 4). Thanks to this system, the following faults are handled manually and a control card is transmitted to the control part of the system, which is designed by means of a cable from the serial port.

With this system, the following faults can be given manually. These;

Fig. 4. Air conditioning training simulator system

In summer position:

- *Compressor valve plates leakage leaking*
- *Four-way valve leaking failure*
- *Condenser blockage failure*
- *Filter blockage failure*
- *Electronic expansion valve malfunction*
- *Capillary blockage failure*
- *Evaporator blockage failure*
- *Defective refrigerant deficiency*
- *Refrigerant surplus failure*
- *Air malfunction in the system*
- *Indoor unit pollution failure*
- *Condenser fan failure*
- *Compressor malfunction.*

In winter position:

- *Compressor valve plates leakage leaking*
- *Four-way valve leaking failure*
- *Condenser blockage failure*
- *Filter blockage failure*
- *Electronic expansion valve malfunction*
- *Capillary blockage failure*
- *Evaporator blockage failure*
- *Defective refrigerant deficiency*
- *Refrigerant surplus failure*
- *Indoor unit pollution failure*
- *Condenser fan failure*
- *Compressor malfunction*

In addition to these faults, the following information is obtained through the control card.

- *Compressor inlet temperature*
- *Compressor outlet temperature*
- *Condenser inlet temperature*
- *Condenser outlet temperature*
- *Evaporator inlet temperature*
- *Evaporator outlet temperature*
- *Storage gas quantity*
- *Compressor input pressure*
- *Compressor outlet pressure*
- *Capacitor input pressure*
- *Condenser outlet pressure*
- *Evaporator inlet pressure*
- *Evaporator outlet pressure*

B. STAGE TWO: MICROCONTROLLER MODULE

If a microcontroller is chosen for an application, this selection should be made to meet the requirements of the application being designed. The purpose of this work is to read the data received from the serial port via the air conditioning module and to communicate with the Wi-Fi module quickly and send this information to a database on the internet. For this reason, the most basic feature of PIC to be selected is that it has serial port communication support and can work at high frequency. It is also important that you have the ability to perform very fast operations.

The dsPIC33EP512MU810 (Figure 5) is used as a microcontroller in the tramped electronic circuit. The microcontroller is directly connected to the Ethernet / Wi-Fi module, RTC-E2, display and RS 232 integration. Also a GPRS integration allows SIM cards to be read and connected internally for later use on the circuit. The designed electronic circuit also uses PLL (Phase Locked Loop). Thanks to this

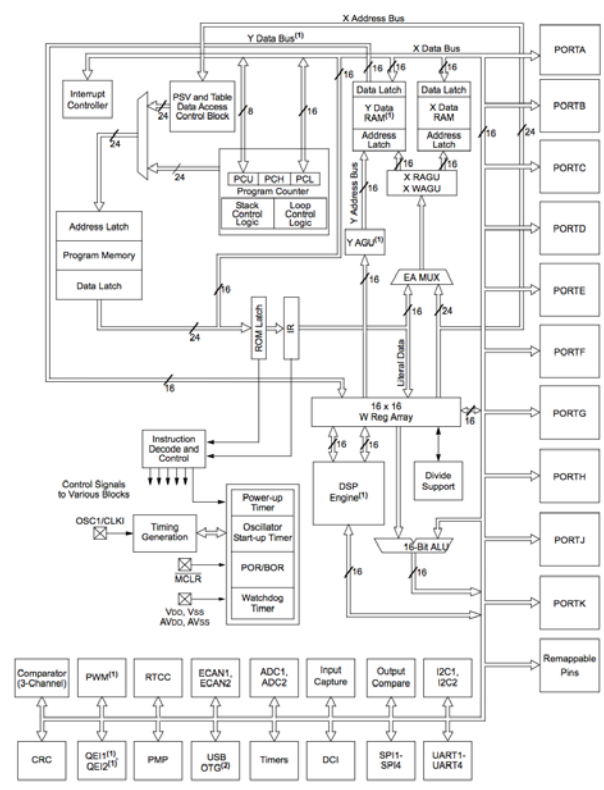

Fig. 5. dsPIC33EP512(MU)810 block diagram [9]

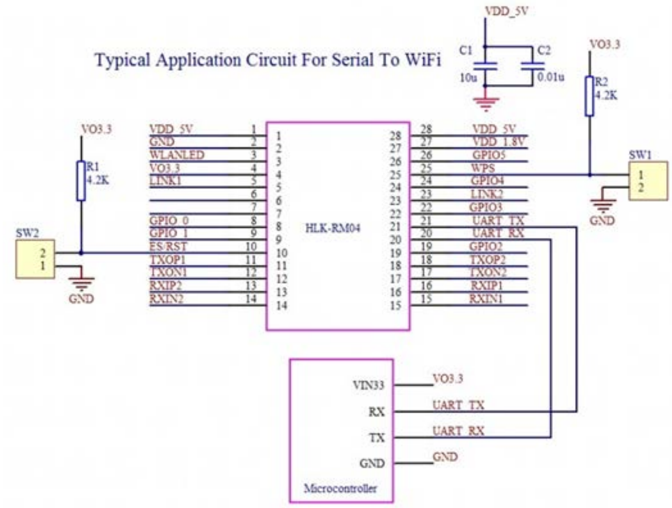

Fig. 6. Application circuit for serial to Wi-Fi.

structure, a stable frequency is produced[10, 11].

In this designed system, the wireless network module is configured[12]. For this, HLK-RM04 was used (Figure 6). This module is an embedded module based on the TCP / IP protocol, serial port, Ethernet, universal serial interface network standard that hosts wireless network. In this way, there is no need to make any configuration on conventional serial devices[13, 14]. In addition, the MPC79410 real time clock (RTC) (Figure 7) integration is used to record incoming data according to the real-time clock. The feature of this integration is that it does not lose its date and time information even if there is a power failure by generating a self-clock signal with the aid of an independent battery and an oscillator with a frequency of 32768 KHz connected to pins X1 and X2 of the integrator[15].

The first part of the designed device (Figure 8) consists of feeding and RS232 connections. In order to avoid the problem of polarity in applying the supply voltage at this stage, a circular connector structure and a bridge diode are used. For RS232 connection, an external RS232 connection is connected and DB9 connector is connected to the integrated output. This connection allows the data is taken from the air conditioning module. Another DB9 connector connected to the Rx and Tx

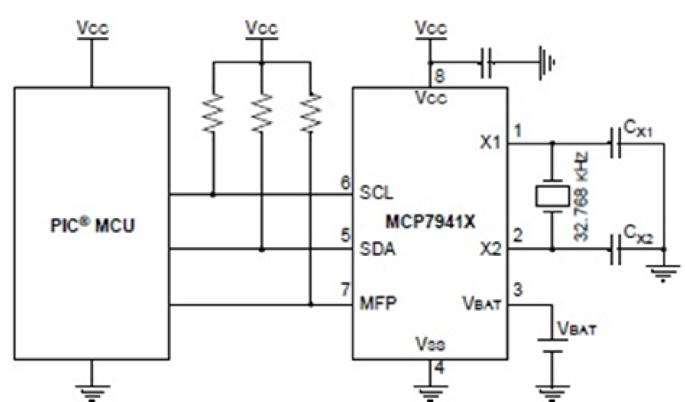

Fig. 7. Application circuit for MPC7910

Fig. 8. Designed circuit

ends of the microcontroller is connected directly so that the PIC integration can be set via the computer.

Finally, the controller, the pressure, the temperature, and the amount of gas from the air conditioner module via the serial port are sent to a database on the internet via a wireless modem via the Wi-Fi module in the system.

C. Stage Tree: Server module

In this part of the work, the data from the system are recorded in a database and the application of the neural network results obtained in chapter III is explained. The monitored data in Micro controller card is transferred to MySQL database server through internet. PHP API executes on the internet server [16]. The recorded data is useful for further analysis and may be useful for data mining. The Fast-Artificial Neural Network Library, a PHP library, was used to evaluate the failure of the experimental work described in Part III. Thus, when the fault information is applied by push messaging method, active users at that moment will beep and send a notification. The system consists of the front-end user interface part, the data filtering and processing part, the data collector part, and the module in which the data is stored. They also communicate with a PHP API (Figure 9). The Admin user (if desired front-end user) interface module supports graphical user interface through web browser with HTML and java script. The module is implemented by angular.js and node.js. The users explore and retrieve the information DB through data filtering and processing module and the information is shown in web page [17].

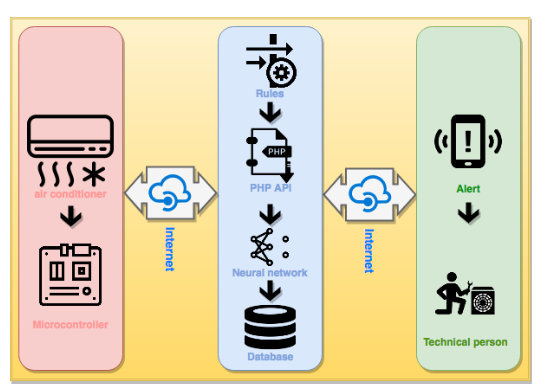

Fig. 9. Server relationship model

D. STAGE FOUR: USER MODULE

An Android application is developed (Figure 10) in the Android Studio using Java[18, 19]. Internet connection permissions are given in it to connect with Wi-Fi. Data from the database (located in MySQL) can be obtained on the mobile phone by clicking the developed Android application on the mobile phone. When the android program is clicked, it connects to URL of PHP API. As a result, PHP API connects with the database and returns the data to the mobile phone [20, 21].

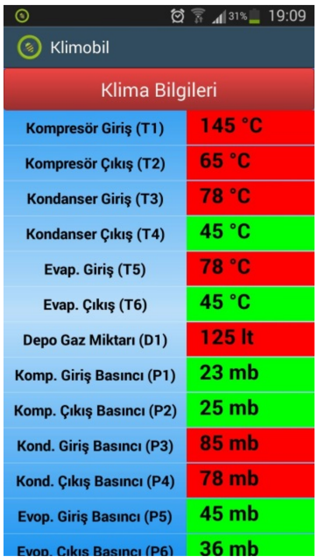

,

Fig. 10. Screen display showing air conditioner data

The developed mobile application also uses "push notification" for instant messaging. Mobile push notifications are an important feature of mobile computing services and they have been widely implemented in mobile applications[22]. Push notification is conceptually an event-based mechanism where remote servers push events, as and when they occur, to smartphone client apps[23]. In particular, it was used to inform the technical staff that the malfunctions that occurred instantaneously and the air conditioning system were out of working values. The Firebase Cloud Messaging (FCM) service is used for this. This is a service that developers use to send push notifications[24]. Using FCM, you can notify a client app that new email or other data is available to sync. You can send notification messages to drive user re-engagement and retention[25].

The mobile software processes the data coming from the server and displays the values other than the nominal values as red and the nominal values as green as above. The data coming from the climate is also prepared graphically according to time. The graphical screen display is shown in Figure 11. In addition, data from the air conditioner is graphically displayed on time, if desired. The graphical screen display is shown in Figure 11.

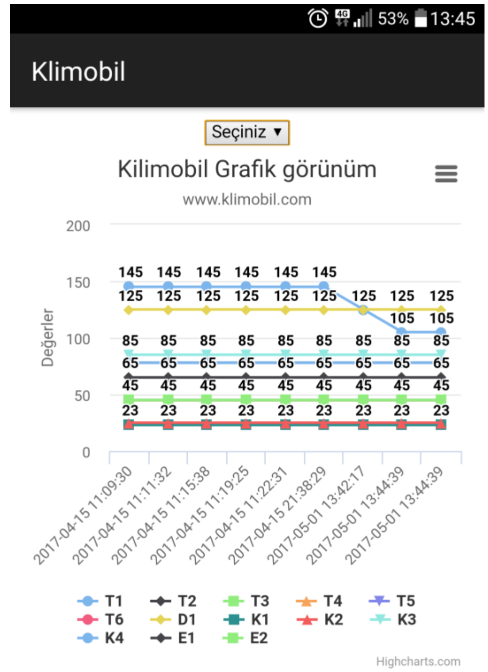

Fig. 11. Screen display of air conditioner data graphically.

III. DIAGNOSING FAULTS WITH NEURAL NETWORKS

The work done in this section was made to create an academically ground for practice. In this study, the malfunction information of an Air-Conditioning Training Simulator device is taken and a wireless network and a server in internet environment are sent to the database and a prediction is made. For this reason, in order to evaluate the detection of such faults by means of a prediction method, sample faults were created by using hardware components from the Air Conditioning Training Simulator and the 1120 sample data were obtained.

The following fault classes have been established for this estimation, and the distributions of these data according to fault classes are given in Table I

Table I. Distribution of data according to occurrence

Evap Fan Failure	64
Evap Clogged	94
Gas Deficient	120
Gas Oversupplied	71
Element of Expansion Failure	47
Condenser Fan Failure	57
Condenser Clogged	146
Normal	521

Multilayer (MLP) neural network classification was performed using this data. Artificial Neural Networks are basic models of computation that resemble the function of a biological network of neurons and are used to solve complex functions in a variety of applications such as design, implementation, visualization, and Neural Network Simulation tools [26-28]. This is the most popular MATLAB Network Toolbox software, along with a lot of software for calculations. This software provides comprehensive support for graphical user interfaces (GUIs) that allow for the design and management of networks. The modular, open and extensible design of the toolbox simplifies the creation of customized functions and networks and transforms the neural network into software scripts called M-code[29, 30].

As can be seen in Figure 12, three different layers of input, hidden and output layers are used in this system. It consists of the sensor data ("Loadcell","KompGirişBasıncı", "KompÇıkışBasıncı","KondGirişBasıncı","KondÇıkışBasıncı,"EvopGirişBasıncı","EvopÇıkışBasıncı","T1","T2","T3","T4","T5","T6","T7","T8") as input layer. Information from the input layer is then processed in a single hidden layer; The output vector is calculated in the failure class (output) layer.

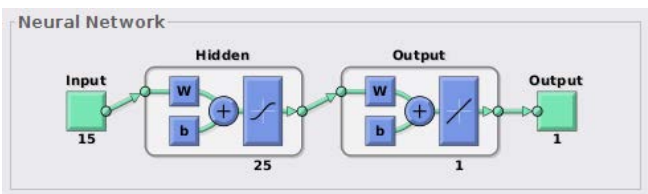

Fig. 12. Network model.

The success of the multilayer perceptron (MLP) Neural Network classification has been researched based on training, validation and test performance. The training performance of the neural network was investigated for different speeds, and the best performance for the Multi-layer network training algorithm was 99.91%.

The best training results were obtained with the Levenberg Marquardt (TrainLM) algorithm. The hyperbolic tangent sigmoid transfer function (Tansing) and Linear transfer function (Purelin) were used to optimize the input layer function. Performance ratio and training speed The best results are obtained with the linear transfer function (Purelin). The number of neurons in the hidden layer was determined by trial and error, and the results were listed for meaningful experiments. Depending on the training and performance indices, the number of layers of hidden neurons was chosen as 25. After running the multilayer perceptron (MLP) Neural Network using optimal parameters, 99.98% training performance and 96.84% test performance were achieved as described in the correlation graphs (Figure 13).

As shown in Figure 14, the multilayer perceptron (MLP) Neural Network algorithm has been successful with learning consisting of 70 iterations. Training was performed by selecting 25 hidden layers, and the other parameters were set to default values. Higher training and test rates indicate that MLP neural networks and Neural Pattern Recognition algorithms can be used safely for classifying failures.

As a result of these evaluations, the data is processed in the Artificial Neural Network layer on the server and this data is sent to the user in the instant notification via the mobile application.

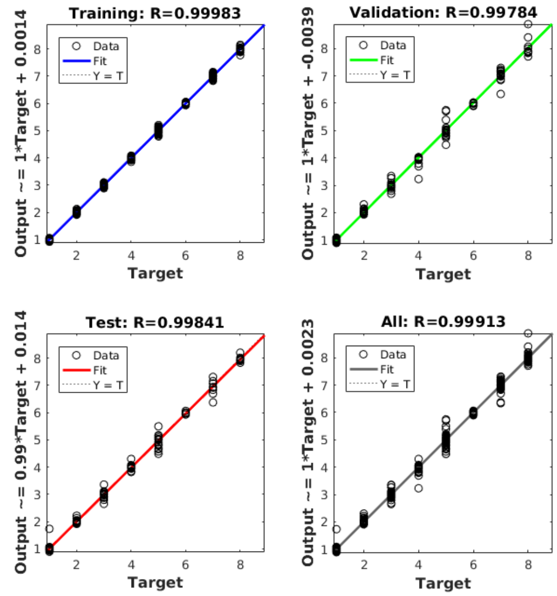

Fig. 13. Correlation Rates for Training, Verification and Test Data.

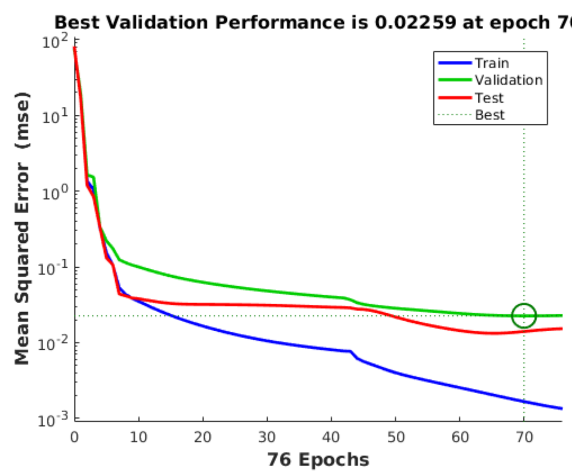

Fig. 14. The best validation performance

IV. CONCLUSION

When studies done in the literature are examined, different hardware components and cards are used for fault detection and different estimation methods are examined for fault detection. This work demonstrates that manufacturers who apply the rapidly developing IOT (Internet of Things) production technologies will be more solution oriented and make faster decisions than other manufacturers. The system itself will no longer make such malfunction decisions. When the devices are connected to each other, the generated data is rapidly transferred to each other through high speed internet support through the software that each device generates its own data and it is possible to make faster and more effective decisions by looking at the results obtained from the data. With these systems, these decisions are transferred to both the personnel at work, the manager who follows the job and all the devices and a synchronized working environment is provided. It is very important that the workforce develops and develops towards this developing technology in air conditioning maintenance and service. Because in the production phase, tasks and responsibilities in all jobs and units are influenced both by human training and by the professionalization of the person. It is unthinkable that this situation does not exist in technical service. It is clear that a system that detects failures before failures can reduce possible material and spiritual losses. However, new business profession will be born. In addition, the development of quality of service, especially in the case of malfunctions, has shown that air conditioning systems will contribute to productivity in workplaces that are heavily used during business processes. The success of the artificial neural network applications in different areas has shown that this work can be successful in predicting and transferring faults that may occur. In addition to achieving the desired outcome with this study, the evaluation of other estimation methods will contribute to both the academic studies and the sector.

REFERENCES

[1] A. Holley. (12.06.2017). *Air conditioning trends and forecast*. Available: https://www.slideshare.net/BSRIA/air-conditioning-trends-and-forecast-anette-meyer-holley-john-updatesv2-edited

[2] F. ÖZEL and M. Z. HANÇER, "Hastanelerde iklimlendirme Sistemleri," *Tesisat Mühendisliği Dergisi,* vol. 89, pp. 27-42, 2005.

[3] C. a. E. Engineering. (12.06.2017). *Achieving the Right Temperature: Diagnosing Faults and Monitoring Efficiency of HVAC Systems*. Available:https://www.cmu.edu/cee/news/news-archive/2016/2016-achieving-the-right-temperature-diagnosing-faults-and-monitoring-efficiency-of-hvac-systems.html

[4] V. Venkatasubramanian, R. Rengaswamy, K. Yin, and S. N. Kavuri, "A review of process fault detection and diagnosis," *Computers & Chemical Engineering,* vol. 27, no. 3, pp. 293-311, 2003/03/15/ 2003.

[5] S. Katipamula and M. Brambley, "Review Article: Methods for Fault Detection, Diagnostics, and Prognostics for Building Systems—A Review, Part I," *HVAC&R Research,* vol. 11, no. 1, pp. 3-25, 2005.

[6] Y. Yu, D. Woradechjumroen, and D. Yu, "A review of fault detection and diagnosis methodologies on air-handling units," *Energy and Buildings,* vol. 82, pp. 550-562, 2014.

[7] B. Yu, D. H. C. Van Paassen, and S. Riahy, "General modeling for model-based FDD on building HVAC system," *Simulation Practice and Theory,* vol. 9, no. 6, pp. 387-397, 2002/05/15/ 2002.

[8] S. Wang and Y. Chen, "Fault-tolerant control for outdoor ventilation air flow rate in buildings based on neural network," *Building and Environment,* vol. 37, no. 7, pp. 691-704, 2002/07/01/ 2002.

[9] Microchip, "dsPIC33EPXXX(GP/MC/MU)806/810/814 - 16-Bit Microcontrollers and Digital Signal Controllers with High-Speed PWM, USB and Advanced Analog," vol. Data Sheets, ed: Microchip, 10/17/2012, p. 24.

[10] G. Leonov and S. Seledzhi, "Design of phase-locked loops for digital signal processors," *International Journal of Innovative Computing, Information Control,* vol. 1, no. 4, pp. 779-789, 2005.

[11] G. Leonov, N. Kuznetsov, and S. Seledzhi, "Nonlinear analysis and design of phase-locked loops," in *Automation Control-Theory and Practice*: InTech, 2009.

[12] Hi-Link. (2016, 12.0.2017). *low-cost embedded UART-ETH-WIFI (Serial - Ethernet - Wireless network) module*. Available: http://www.hlktech.com/upfile/2016/07/17/20160717214110_760.pdf

[13] Z. M. Kalarthi, "A review paper on smart health care system using Internet of Things," *International Journal of Research in Engineering and Technology (IJRET),* vol. 5, pp. 80-3, 2016.

[14] P. S. N. Reddy, K. T. K. Reddy, P. A. K. Reddy, G. K. Ramaiah, and S. N. Kishor, "An IoT based home automation using android application," in *Signal Processing, Communication, Power and Embedded System (SCOPES), 2016 International Conference on*, 2016, pp. 285-290: IEEE.

[15] S. Şerbetli, "Fotovoltaik Panellerde Güç Üretiminin Gerçek Zamanlı Olarak İzlenmesi Ve Verilerin Saklanması," Master, Fen Bilimleri Enstitüsü / Elektrik Eğitimi Anabilim Dalı, Marmara Üniversitesi, 2016.

[16] J. Shah and B. Mishra, "Customized IoT enabled Wireless Sensing and Monitoring Platform for preservation of artwork in heritage buildings," in *2016 International Conference on Wireless Communications, Signal Processing and Networking (WiSPNET)*, 2016, pp. 361-366.

[17] J. H. Park, J. Chung, and S. Y. Chae, "Design of IoT information System," 2016.

[18] J. F. DiMarzio, *Beginning Android Programming with Android Studio*. John Wiley & Sons, 2016.

[19] J. DiMarzio, "Setting Up Android Studio," in *Android Studio Game Development*: Springer, 2015, pp. 1-8.

[20] O. A. Ibrahim and K. J. Mohsen, "Design and implementation an online location based services using Google maps for android mobile," *International Journal of Computer Networks and Communications Security (CNCS),* vol. 2, no. 3, pp. 113-118, 2014.

[21] S. Kumari, M. Yadav, and S. R. Kumari, "Database Connection Technology," *International Journal,* vol. 8, no. 5, 2017.

[22] J. Ding, W. Song, and D. Zhang, "An Approach for Modeling and Analyzing Mobile Push Notification Services," in *Services Computing (SCC), 2014 IEEE International Conference on*, 2014, pp. 725-732: IEEE.

[23] I. Warren, A. Meads, S. Srirama, T. Weerasinghe, and C. Paniagua, "Push notification mechanisms for pervasive smartphone applications," *IEEE Pervasive Computing,* vol. 13, no. 2, pp. 61-71, 2014.

[24] M. Ahmadi, B. Biggio, S. Arzt, D. Ariu, and G. Giacinto, "Detecting Misuse of Google Cloud Messaging in Android Badware," in *Proceedings of the 6th Workshop on Security and Privacy in Smartphones and Mobile Devices*, 2016, pp. 103-112: ACM.

[25] Google. (12.05.2017, 12.06.2016). *Firebase Cloud Messaging*. Available: https://firebase.google.com/docs/cloud-messaging/

[26] J. J. Hopfield, "Artificial neural networks," *IEEE Circuits and Devices Magazine,* vol. 4, no. 5, pp. 3-10, 1988.

[27] J. E. Dayhoff and J. M. DeLeo, "Artificial neural networks," *Cancer,* vol. 91, no. S8, pp. 1615-1635, 2001.

[28] B. Yegnanarayana, *Artificial neural networks*. PHI Learning Pvt. Ltd., 2009.

[29] A. Cochocki and R. Unbehauen, *Neural networks for optimization and signal processing*. John Wiley & Sons, Inc., 1993.

[30] J. Hines, L. H. Tsoukalas, and R. E. Uhrig, *MATLAB supplement to fuzzy and neural approaches in engineering*. John Wiley & Sons, Inc., 1997.

BIOGRAPHIES

Hüseyin Yüce was born in Sivas in 1972. He completed his undergraduate, graduate and doctorate studies at Marmara University. He works as a faculty member in the Faculty of Technology, Mechatronics Engineering. He works in computer programming, artificial intelligence, deep learning, embedded systems, image processing and Nano technology.

Köksal Avcı was born in Istanbul in 1976. He graduated from Marmara University Electronics and Computer Teaching Department in 1999. He has been working as a teacher of information technology in the Ministry of National Education. Köksal is about to complete his master's thesis at the Marmara University Institute of Pure and Applied Sciences.

THE JOURNAL OF COGNITIVE SYSTEMS
VOLUME 02 NUMBER 01 JUNE 2017

COGNITIVE SYSTEMS AND QUANTUM COMPUTATION

Deniz Türkpence[1]

[1] Istanbul Technical University, Istanbul, Turkey

This review presents an overview of cognitive systems, quantum phenomena and possible connections between them. The focus will be the artificial cognitive systems and briefly touch the discussion of possible benefits from quantum counterparts. The non-classical features of Quantum Theory introduced as quantum resources which enables possible speed ups or advantages over classical computational tasks. Quantum computation is introduced as a powerful computational tool over its classical counterparts by also covering possible applications of cognitive phenomena in the framework of quantum cognition. Also different attempts in order to implement decision making processes for cognitive purposes mentioned.

Index Terms — Quantum computation, quantum machine learning, cognitive systems, quantum resource

I. INTRODUCTION

COGNITIVE science is an inter-disciplinary study of decision making, intelligence including artificial intelligence and artificial neural networks and also human memory linguistics and anthropology [1]. On the other hand, quantum cognition adopts quantum probability theory instead of classical probability theories derived from Kolmogorov axioms [2] obey the Boolean axioms of logic. Since the quantum logic is able to explain some discrepancies between experiment and the classical probability principles such as in the 'disjunction effect' [3]; quantum logic becomes a generalization of classical logic and quantum probability theory.

Cognition can be defined as the ability to process information of perception knowledge acquired through experience. Though perception and experience look like humanoid concepts, the term 'learning' is widespread used for algorithmic processes as 'machine learning' in the context of artificial intelligence which is a field of computer science deals with intelligent machines mimic human behaviors. The term artificial intelligence (AI) first coined by john McCarthy in 1956 in a workshop referred to as the official birth of artificial intelligence [4]. Frank Rosenblatt developed 'perceptron' an early artificial neural network based on a two-layer computer learning network [5]. Today AI finds applications of our everyday life from pattern recognition implementations, driverless cars to the humanoid robots mimicking physical human actions. The progress of machine learning algorithms advances the AI current state of art as an underlying fact.

Since the volume of processed global data has reached a persistent annual increment [6] the idea to benefit the potential of quantum computing and information emerges by the physics society [7]. To this end, there are several proposals exploring the gains of unification of machine learning algorithms with quantum computing, particularly with efforts to develop quantum versions of artificial neural networks[8-10]. Another proposal is to reformulate the machine learning subroutines in order to implement on a quantum computer [11-13]. This review presents a general survey of possible proposals to relate machine learning in the context of cognitive systems. Future prospects and open problems also addressed.

II. WHY QUANTUM?

Quantum theory is the theory (QT) of matter and energy based on the quantization nature with successful mathematical descriptions. The historical development of QT is full of debates and scientific discussions due to its counter-intuitive nature [14]. Today, QT appears to be one of the most successful theories ever with the large number of experimental verifications. Moreover, the subject of early discussions such as 'quantum superposition' or 'quantum entanglement' is now resources of current quantum technologies. Quantum superposition is the existence of linear combinations of distinct eigenstates representing a physical system. Superposition is a direct consequence of Schrödinger equation which is a differential equation representing the temporal evolution of a quantum system as wave mechanics formulation. Though this fact, Erwin Schrödinger criticized the result of his own equation by quoting a cat in a superposition of states 'alive' and 'dead' in which later become famous as Schrödinger's cat [15]. These results triggered an enhancement of already existing discussion in the physics community about the interpretations of QT including uncertainty, measurement problem and wave function collapse [16-17]. One discussion side embraced QT with its own counter-intuitive nature by describing a quantum system

Manuscript received May 9, 2017; accepted May 25, 2017.
Corresponding author: Deniz Türkpence (E-mail: dturkpence@itu.edu.tr; ORCID® ISNI: 0000-0002-8491-586X).
Digital Object Identifier:

as not corresponding to a physical quantity before a measurement. This view of QT is known as Copenhagen interpretation devised by Neils Bohr and Werner Heisenberg reflecting the uncertain and probabilistic nature of QT. On the other hand, Einstein and Schrödinger refused the probabilistic nature or wave function collapse and tried to express the results in a deterministic way. In 1935 Einstein attacked the fundamentals of QT with a paper interrogating the completeness of QT by introducing a thought experiment expressing that by the admittance of the validity of Copenhagen interpretation QT is in a clear contradiction with locality, special relativity and causality principles [18]. John Bell invented an inequality in 1964
[19] which is not possible to be violated under Einstein's deterministic assumptions of QT. By this inequality discussions were able to be carried into the laboratory. Experimental studies examining the inequalities resulted by the violations of the inequalities [20]. By these results non-local correlations of QT , 'quantum entanglement' [21] has been experimentally proven. Quantum entanglement is now being used as a quantum resource and enables quantum teleportation [22], quantum dense coding [23] and quantum cryptography [24] possible. Non-classical quantum resource is not the only compelling reason for quantum technologies. In 1960's Gordon Moore noticed that the number of transistors in a circuit doubles every two years [25].

According to this observation the number of atoms represent one bit of information decrease logarithmically means that miniaturization process of electronic devices will end up with the entrance of the quantum region with a few or less atoms where the classical circuit theory is no longer valid [26]. By these facts, first arguments about implementing computational logic governed by quantum systems which is known as the first building blocks of quantum computation coined by Paul Benioff [27]. A milestone appeared by Richard Feynman's report based on the idea of the potential of the efficient simulation of quantum systems could be implemented by other quantum systems [28]. The first quantum logical algorithm reported by David Deutsch in 1985 considering the solution of a decision problem with a speed up over classical algorithms by exploiting quantum superposition principle [29]. A breakthrough of interest to quantum computation occurred after the introduction Shor's factoring algorithm which can factorize long digit prime numbers in polynomial time [30] followed by Simon's algorithm [31] for period finding in polynomial time and Grover's search algorithm in an unstructured database [32].

Though quiet much number of quantum algorithms developed to date, these algorithms are mostly the variants of the quantum algorithms considered above. The reasons of the difficulty of developing novel pure quantum algorithms are twofold. First, developing a pure quantum algorithm is not sufficient alone since the necessity to have better performance over any classical algorithm among its classical counterparts. Second, since the developers of the algorithms live in a classical world, it's difficult to lift the barriers arising from the classical intuitions to reach pure quantum algorithms. For a comprehensive introduction to quantum computation see [33-34].

Undoubtedly, a natural question arises about the possibility of building a feasible quantum computer. There are several physical systems as candidates to implement quantum algorithms [35]. Di Vincenzo reported some criterias for quantum systems should fulfill in order to be

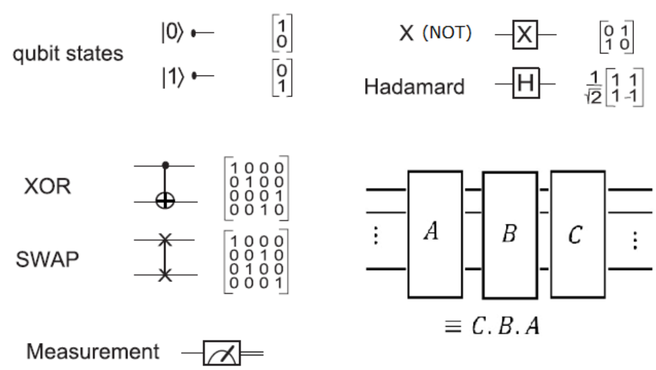

Fig.1 Circuit and matrix representations of some quantum logic gates. Each line represents quantum bits while double lines (after measurement) represent classical bits. Time flows from left to right in a quantum circuit and matrix multiplication order to the qubit states is from right to left.

considered as a universal quantum computer [36]. After two decades of research experience no single physical quantum system appears to fulfill these criterias in a complete manner. However, hybrid systems such as semi-conductor and superconductor systems are promising for future applications [37-38].

III. QUANTUM COMPUTATION

Quantum computation (QC) [33-34] is a computational method using the mathematical abstractions defining the nature of quantum mechanics. The elementary processing unit of QC is quantum bits or 'qubits' in short, defined by a unit bi-dimensional vector

$$|\psi\rangle = \alpha|0\rangle + \beta|1\rangle \qquad (1)$$

in a $\mathbb{C}^2$ complex vector space where $|0\rangle$ and $|1\rangle$ are the computational basis in dirac notation and $\alpha, \beta \in \mathbb{C}^2$ such that $|\alpha|^2 + |\beta|^2 = 1$. Computational basis are represented by column vectors as

$$|0\rangle = \begin{bmatrix}1\\0\end{bmatrix} \quad , \quad |1\rangle = \begin{bmatrix}0\\1\end{bmatrix} \ . \qquad (2)$$

Larger complex vector spaces required in order to define multi-qubit systems in the context of QC. For instance, N qubit system can be expressed as

$$|\Phi\rangle = |\phi_1\rangle \otimes |\phi_2\rangle \otimes .. \otimes |\phi_N\rangle \tag{3}$$

or as $|\Phi\rangle = |\phi_1\phi_2..\phi_N\rangle$ in short where $\otimes$ stands for a tensor product of vectors.

Logical operators acting on computational basis of N qubits are the $2^N \times 2^N$ dimensional unitary operators represented by unitary matrices U, obeying $U^\dagger U = \mathbb{1}$ where $U^\dagger$ is the transpose conjugate and $\mathbb{1}$ is the unitary matrix with a convenient dimension. Fig.1 depicts the single and multi-qubit gates and a circuit representation and relevant symbols of quantum circuits.

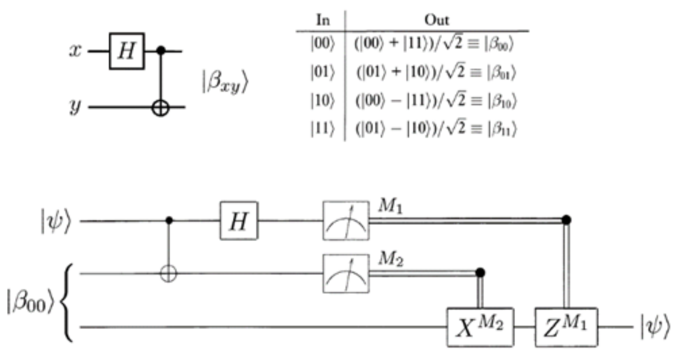

Fig.2. Bell state generator (top panel) and the quantum teleportation circuit (bottom panel). Bell states are the entangled states and are widely used in QC circuits.

As considered before, quantum superposition is one of the main resources of QT which makes QC more powerful. Benefiting quantum superposition of QC processes is known as quantum parallelism. Therefore Hadamard operator H, is of central importance since its action is to put single computational basis $|0\rangle$, $|1\rangle$ into superposition such as

$$H|0\rangle = \frac{1}{\sqrt{2}}(|0\rangle + |1\rangle) \quad , \quad H|1\rangle = \frac{1}{\sqrt{2}}(|0\rangle - |1\rangle). \tag{4}$$

Also multi-qubit gates are necessary to implement multi-qubit operations. For instance, a two- qubit quantum gate C-NOT gate can be represented by a generalization of XOR gate with the action $|A,B\rangle \rightarrow |A, B\oplus A\rangle$. Then the effect of C-NOT gate can be represented by actions $|00\rangle \rightarrow |00\rangle$, $|01\rangle \rightarrow |01\rangle$, $|10\rangle \rightarrow |11\rangle$ and $|11\rangle \rightarrow |10\rangle$. Here the first qubit is the control qubit and the second qubit is the target qubit. If the state of the control qubit is 0 then the gate leaves the target qubit left alone, if the target qubit is 1 then X (Not gate) is applied to the target qubit. In fact this is a conditional operation and the state of the target qubit flipped depended on the condition of the control qubit. These conditional operations can be generalized by any two-qubit operator U and the matrix representation can be decomposed as

$$CU = |0\rangle\langle 0| \otimes \mathbb{1} + |0\rangle\langle 0| \otimes U \tag{5}$$

where $\langle .|$ is the transposition of any qubit state. Another important two-qubit gate is the swap gate in which swaps the two qubit state. The action of this gate can be summarized as $|01\rangle \rightarrow |10\rangle$, $|10\rangle \rightarrow |01\rangle$ for instance. Another gate operation worth mentioning is the 'Bell state generator' which is a two-qubit operation with an Hadamard gate applies to the first qubit followed by a C-Not gate to the both qubits. By this operation, entangled states are obtained for different possible input states (Fig.2 top panel). A general expression for Bell states is

$$|\beta_{xy}\rangle \equiv \frac{|0,y\rangle + (-1)^x|1,\bar{y}\rangle}{\sqrt{2}}. \tag{6}$$

A simple application of entangled states is the quantum teleportation circuit (Fig.2 Bottom panel) which teleports an unknown quantum state from one qubit to another one.

The final stage of the quantum computational tasks is the measurement. According to the measurement postulate of QT, quantum measurements are described by a set of measurement operators $\{M_m\}$ acting on the states of the relevant systems being measured. Here the index m is the measurement outcome in the experiment where the probability result m occurs is

$$p(m) = \langle\psi|M_m^\dagger M_m|\psi\rangle. \tag{7}$$

The state of the system after the measurement is

$$|\varphi'\rangle = \frac{M_m|\psi\rangle}{\sqrt{\langle\psi|M_m^\dagger M_m|\psi\rangle}}. \tag{8}$$

Here, the linear sum of measurement operators is equal to unity $\sum_m M_m^\dagger M_m = I$ implying that the probabilities sum to one. Before the measurement the evolution of the system is unitary which means that the system has no contact with the environment. Measurements are the interactions with the environment or the measurement apparatus in which the details of the measurement process is the out of the scope of QC.

IV. TOWARDS QUANTUM COGNITIVE COMPUTATION

Direction of computer science evolved more rapidly towards cognitive computation in the past decade. Cognitive features of a computer, in other words ability to learn and implementing decisive processes will be a more efficient assistant for humans. IBM researchers underline the shift in technology with new advances with the cognitive abilities by their experience based on the first cognitive system Watson [39]. According to IBM Watson CTO, quantum computing would advance artificial intelligence by orders of magnitude [40]. By this point of view, recent ideas on improving machine learning algorithms by exploiting the advantages of quantum computing have been reported [41-45]. Clustering unstructured or sorting labeled data are the central problems of unsupervised or supervised learning which are important topics of machine learning.

Quantum version of specific classical algorithms for pattern classification has been reported for different goals. For instance swap test [46] was introduced in order to identify the similarity between two quantum states. Inspired by the swap test Lloyd et al proposed a routine to recover classical distance between two vectors via quantum measurement [47]. On the other hand, a pure quantum pattern recognition aimed algorithm was developed by Trugenberger [44]. The procedure was based on the measurement of hamming distance between two binary quantum states. Lloyd et al also developed a quantum support vector machine for supervised machine learning [48] and quantum principle component analysis [49] as applying classical ML procedures to quantum register. Beyond the efforts of implementing QC tasks in terms of cognitive duties a comprehensive theory of quantum learning is still missing. Therefore cognitive studies exploiting the advantages of QT make an active research area including the past two decades' useful discussions about the efforts on understanding of origin of human consciousness linked by QT [50].

CONCLUSIONS

The current direction of quantum cognitive processes appears to be divided into two main paths; first, application of cognitive processes to quantum computation with already existing quantum algorithms; second, implementing cognitive tasks to quantum systems. Though yet there is no current convincing theory of quantum learning, the capacity of quantum registers with valuable quantum resources makes quantum cognitive systems a promising candidate to strengthen the capacity of cognitive systems.

REFERENCES

[1] J. R. Busemeyer, P.D. Bruza, *Quantum Models of Cognition and Decision*, Cambridge University Press, 2012 .

[2] A. N. Kolmogorov, *Foundations of the theory of probability,* Chealsea publishing, New York, 1993.

[3] A. Tversky and E. Shafir, "The disjunction effect in choice under uncertainity", *Psychological Science*, vol. 3, pp. 305-309, 1992.

[4] V. Rajaman, "John McCarthy –Father of artificial intelligence " *Asia Pacific Mathematics News Letter*, vol. 4 No. 3 July, 2014.

[5] Rosenblatt F., "The perceptron : A Probabilistic model for information storage and organization in the brain", *Psychological Review* vol. 65 ,pp. 386-408, 1958.

[6] M. Hilbert and P. López, "The world's technological capacity to store, communicate, and compute information", Science vol. 332, , pp. 60–65, 2011.

[7] F. Petruccione et. al., "An Introduction to quantum machine learning", *Contemporary Physics,* vol. 56 No. 2 , pp. 172-185, 2015.

[8] G.G. Rigatos and S.G. Tzafestas, "Neurodynamics and attractors in quantum associative memories", Integr. Comput-Aided Eng. Vol. 14, pp. 225–242, 2007.

[9] E.C. Behrman and J.E. Steck, "A quantum neural network computes its own relative phase", IEEE Symposium Series on Computational Intelligence , Singapore, April 15–19, 2013.

[10] S. Gupta and R. Zia, "Quantum neural networks", J. Comput. Syst. Sci. Vol. 63 , pp. 355–383, 2011.

[11] O. S. Lloyd, M. Mohseni, and P. Rebentrost, "Quantum algorithms for supervised and unsupervised machine learning", preprint arXiv:1307.0411 (2013).

[12] P. Rebentrost, M. Mohseni, and S. Lloyd, *Quantum support vector machine for big data classification*, Phys. Rev. Let. Vol. 113 , pp. 130503-1–130503-5, 2014.

[13] H. Neven, V.S. Denchev, G. Rose, and W.G. Macready, "Training a large scale classifier with the quantum adiabatic algorithm", preprint arXiv:0912.0779 , 2009.

[14] J. Mehra, H. Rechenberg ; *The historical development of quantum theory,* Springer-Verlag, New York , 1982.

[15] E. Schrödinger, "The present situation in quantum mechanics", *Naturwissenschaften*, vol. 23, 807-823, 1935.

[16] P. E. Vermaas., *Philosopher's understanding of quantum Mechanics*, 1st ed., Cambridge University Press., New York, 1999.

[17] J. Baggot, *Beyond the measure*, 1st ed.., Oxford University Press., New York, 2004.

[18] A. Einstein., B. Podolsky, N. Rosen, "Can Quantum mechanical description of physical reality be considered complete?", *Physical Rewiew*, vol. 47,pp. 777-780, 1935.

[19] J. S. Bell, "On the Einstein-Podolsky-Rosen paradox", *Physics*, vol. 1, 195, 1964.

[20] A. Aspect, J. Dalibard, G. Roger, "Experimental test of Bell's Inequalities using time-varying analyzers", *Phys. Rev. Lett*., vol. 49, pp. 1804–1807, 1982.

[21] K. Horodecki et al, Quantum entanglement, Rev. Mod. Phys. Vol. 81, 865, 2009.

[22] C.H. Bennet, G. Brassard, W. Wooters , "Teleporting an unknown quantum state via dual classical EPR channels", *Phys. Rev. Lett*., vol. 70, 1895-1899, 1993.

[23] C.H. Bennet, S.J. Wiesner, "Communication via one and two-particle operators on Einstein-Podolsky-Rosen states", *Phys. Rev. Lett.* Vol. 69, pp. 2881-2884, 1992.

[24] C.H. Bennet, G. Brassard, "Quantum cryptography: Public key distribution and coin tossing", *In Proceedings of IEEE International conference on computers systems and signal processing*, pp. 175-179, 1984.

[25] G. E. Moore, "Cramming more components onto integrated circuits", *Electronics magazine*, vol. 38, 1965.

[26] C. P. Williams, S. H. Clearwater, *Explorations in Quantum computing*, Springer, 1998.

[27] P. Benioff, "The computer as a physical system: a microscopical quantum mechanical Hamiltonian model of computers as represented by Turing Machines", *J. Stat. Phys. Vol.* **22** , 563.

[28] R. P. Feynman, "Simulating physics with computers, International Journal of Theoretical Physics", vol. 21, pp. 467-488, 1982.

[29] D. Deutsch, "Quantum theory, the Church-Turing pinciple and the universal Quantum Computer", *Proc. R. Soc. Lond. A*, vol. pp. 400, 97-117, 1985.

[30] P.W. Shor, "Fault-tolerant quantum computation. In Proceedings", *37th Annual Symposium on Fundementals of Computer Science*, IEEE Press, Los Alamitos CA, pp. 56-65, 1996.

[31] D.R. Simon,"On the power of quantum computation", Foundations of Computer Science, 1996 Proceedings., 35th Annual Symposium on: 116–123, retrieved 2011-06-06.

[32] L. K. Grover, Quantum mechanics helps in searching a needle in a haystack, Phys. Rev. Lett. vol. 79, 325, 1997.

[33] M. A. Nielsen, I. L. Chuang, *Quantum computation and quantum information*, 2nd ed., Cambridge University Press, Cambridge, 2000.

[34] http://www.theory.caltech.edu/~preskill/ph219/index.html

[35] M. Nakahara , T. Ohmi , *Quantum Computing from linear algebra to physical realizations*, 1st ed., Taylor &Francis, Osaka, 2008.

[36] D. P. DiVincenzo, "The physical implementation of quantum computation", Fortschr. Phys., vol. 48, pp. 771-783, 2000.

[37] Y-P Shim, C. Tahan, "Semi conductor inspired design principles for superconducting quantum computing, *Nat. Com*. vol. 7, pp. 11059, 2016.

[38] G. de Lange et al, "Realizations of microwave quantum circuits using hybrid superconducting-semi conducting nano wire Josephson elements", Phys. Rev. Lett. vol. 115, pp. 127002, 2015.

[39] F. Jabr, "Clever chip: IBM's cognitive computer works like a brain", vol. 211, pp. 20, 2011.

[40] https://www.ibm.com/watson/products.html

[41] E. C. Behrman and J. E. Steck, "A quantum neural network computes its own relative phase", *IEEE Symposium Series on Computational Intelligence* , Singapore, April 15–19, 2013.

[42] S. Gupta and R. Zia, "Quantum neural networks", *J. Comput. Syst. Sci.* 63 , pp. 355–383, 2001.

[43] D. Ventura and T. Martinez, "Quantum associative memory", *Inform. Sci*. 124 , pp. 273–296, 2000.

[44] C. A. Trugenberger, "Quantum pattern recognition", Quant. Inform. Proc. 1 , pp. 471–493, 2002.

[45] R. Schützhold, "Pattern recognition on a quantum computer", *Phys. Rev. A* , vol. 67, pp. 062311, 2003.

[46] H. Buhrman, R. Cleve, J. Watrous, and R. DeWolf, "Quantum fingerprinting", *Phys. Rev. Lett*. vol. 87, 2001, pp. 167902, 2001.

[47] S. Lloyd, M. Mohseni, and P. Rebentrost, "Quantum algorithms for supervised and unsupervised machine learning", preprint arXiv:1307.0411 , 2013.

[48] P. Rebentrost, M. Mohseni, and S. Lloyd, "Quantum Support Vector Machine for Big Data Classification" *Phys. Rev. Lett*., vol. 113, pp. 130503, 2014.

[49] M. Mohseni, P. Rebentrost, and S. Lloyd, "Quantum principle component analysis", Nat. Comm. vol. 10, pp. 631-633, 2013.

[50] J. A. Tuszynski, *Emerging physics of consciousness* , Springer, 2006.

BIOGRAPHY

Deniz Türkpençe obtained his BSc degree in physics from Ondokuz Mayis University in 2000. He obtained his MSc. degree in 2007 followed by research assistantship and PhD in Physics Department of Ondokuz Mayis University. One year experimental part took in place in Dortmund Technical University 2010-2011 in Germany. He obtained his PhD in 2013, followed by starting researches as Post-Doc in Koc University. His research interests are Quantum optics including Cavity-QED and open quantum systems, Quantum Computation and Quantum Information theory. He is currently in Istanbul Technical University as a Post-Doc.

THE JOURNAL OF
COGNITIVE SYSTEMS

an international, peer-reviewed
indexed, and open-access periodical

PUBLICATION ETHICS

All who participate in producing The Journal of Cognitive Systems conduct themselves as authors, reviewers, editors, and publishers in accord with the highest level of professional ethics and standards. Plagiarism or self-plagiarism constitutes unethical scientific behaviour, and is never acceptable. By submitting a manuscript to this journal, each author explicitly confirms that the manuscript meets the highest ethical standards for authors and co-authors. The undersigned hereby assign(s) to The Journal of Cognitive Systems (JCS) copyright ownership in the above paper, effective if and when the paper is accepted for publication by JCS, and to the extent transferable under applicable national law. This assignment gives JCS the right to register copyright to the paper in its name as claimant, and to publish the paper via any print or electronic medium.

Authors, or their employers, in the case of works made for hire, retain the following rights.

+ all proprietary rights other than copyright, including patent rights
+ the right to make and distribute copies of the Paper for internal purposes
+ the right to use the material for lecture or classroom purposes
+ the right to prepare derivative publications based on the Paper, including books or book chapters, journal papers, and magazine articles, provided that publication of a derivative work occurs subsequent to the official date of publication by JCS.
+ the right to post an author-prepared version or an official version (preferred version) of the published paper on an internal or external server controlled exclusively by the author/employer, provided that (a) such posting is non-commercial in nature, and the paper is made available to users without charge; (b) a copyright notice and full citation appear with the paper, and (c) a link to JCS's official online version of the abstract is provided using the Document Object Identifier (DOI) link

THE JOURNAL OF COGNITIVE SYSTEMS

an international, peer-reviewed, indexed,
and open-access periodical

VOLUME 02, NUMBER 01

JUNE 2017

CONTENTS

www.dergipark.gov.tr/jcs

ISSN 2548-0650